Title: Comparative analysis of tardigrade locomotion across life stage, species, and pharmacological treatment

Running Title: Quantification of tardigrade locomotion

Authors: Emma M. Anderson, Sierra G. Houck, Claire L. Conklin, Katrina L. Tucci, Joseph D. Rodas, Kate E. Mori, Loriann J. Armstrong, Virginia B. Illingworth, Te-Wen Lo, Ian G. Woods*

Affiliation: Department of Biology, Ithaca College, Ithaca, New York, USA
*correspondence: iwoods@ithaca.edu

Key words: tardigrade, locomotion, gait analysis

Abstract

Animal locomotion requires precise coordination between the central and peripheral nervous systems, between sensory inputs and motor outputs, and between nerves and muscles. Therefore, analysis of locomotion provides a broad and sensitive readout of nervous system function and dysfunction. Tardigrades, the smallest known walking animals, coordinate movement of their eight legs with a relatively simple nervous system. As such, tardigrades are an attractive model for neuronal control of limb-driven locomotion. Here, we developed tools for automated tracking of tardigrade locomotion in an unconstrained two-dimensional environment, for quantification of multiple parameters of individual leg movements, and for measuring interleg coordination. We use these tools to analyze >13,000 complete strides in >100 tardigrades, and found evidence for preferred walking speeds and distinct step coordination patterns associated with those speeds. In addition, the rear legs of tardigrades, although they have distinct anatomy and step kinematics, were nonetheless incorporated into overall patterns of interleg coordination. Finally, comparisons of tardigrade locomotion across lifespan, between species, and between pharmacological treatments suggested that neuronal regulation of high-level aspects of walking (e.g. speed, turns, walking bout initiation) operate independently from circuits controlling individual leg movements and interleg coordination.

Introduction

Movement is a defining feature of animals, and is essential for survival and reproduction (Bidaye et al., 2018). Animals move to find food, mates, favorable conditions in shifting environments, and to escape predation. As movement is highly optimized and a primary

determinant of morphology and physiology (Alexander, 2006; Dickinson et al., 2000), quantitative analysis of movement can enable insights into key features of an animal's form and function.

Movement requires coordination between the peripheral and central nervous systems, signaling between nerves and muscles, and response to external and internal cues (Bidaye et al., 2018; Miller et al., 2012; Nirody, 2021), and is a sensitive indicator of nervous system function (Dietz, 1997; Gibson and Stork, 2021). For example, walking ability predicts healthspan and life expectancy in elderly humans, and abnormal gait can reveal neurological conditions before clinical diagnoses (Giladi et al., 2013; Pirker and Katzenschlager, 2017). Similarly, movement analysis can uncover the etiology of many pediatric disorders (Wilson and Keener, 2018), and aid in diagnosis of neurological dysfunction in animals (Struble and Gibb, 2022).

Appendage-based movement in vertebrates involves billions of neurons in the central and peripheral nervous systems, making a circuit-level understanding of locomotion a major challenge. Simpler or smaller animals could offer more tractable models, but most microscopic animals move via axial propulsion with undulating or peristaltic movements rather than via alternating limbs. Named for their slow, stepping movements, tardigrades are an exception to this trend. Tardigrades generate appendicular locomotion with a relatively simple nervous system: their bodies consist of < 2000 cells in species where cell number has been measured, and only a few hundred of these cells are neurons (Arakawa et al., 2016; Gross et al., 2019; Mayer et al., 2013; Møbjerg et al., 2011). Tools for genetic manipulation are actively being developed for tardigrades (Goldstein, 2022) making them a promising system to investigate the genetics and neuromuscular biology underlying appendicular locomotion.

To establish tardigrades as a model for locomotor function and dysfunction, we developed open-source tools to track freely-moving individuals, and to quantify planar walking, single-leg stepping, and interleg coordination. We extended previous tardigrade locomotion analyses (Nirody et al., 2021) by including exploratory behavior at large temporal and spatial scales, demonstrating preferences in interleg coordination at different speeds, analyzing coordination between rear and lateral legs, and comparing locomotion across life stages, species, and pharmacological treatments.

Methods

Tardigrade culture

Hypsibius exemplaris (Gąsiorek et al., 2018) were obtained from a commercial source (Sciento, Manchester, England, strain Z151) and maintained in the laboratory in 50 mm Petri dishes coated with 2% agar and filled with 5 mL Poland Spring water. Cultures were refreshed

every 1-2 weeks by replacing the water and adding 5 drops of fresh algae for food (*Chlorococcum*, initially obtained from Carolina Biological Supply, Burlington, NC, USA, catalog 152091, and cultured following procedures from the supplier). New tardigrade stocks were generated every 2-4 weeks by transferring 10-15 adult tardigrades to new agar-coated dishes and adding fresh algae.

Videos of tardigrade locomotion

To quantify tardigrade locomotion, we transferred individuals to empty 35 mm Petri dishes freshly coated with 2% agarose, and filled each dish with 1 mL of Poland Spring water after transfer. Optimal agarose concentration was determined by testing a range between 1% and 3%. At high concentrations, tardigrades frequently lost their grip on the substrate and were unable to walk, whereas lower substrate stiffness is associated with slower movement and compensatory changes in stepping patterns (Nirody et al., 2021). Tardigrades were filmed at 33 Hz under the 10X objective on an inverted microscope with an attached camera (AmScope MD310B-BS). During filming (AmScopeAmLite v3.26.2023), we moved the stage only when necessary to keep the tardigrade in the video frame, thereby maximizing the time during which the background remained stationary. After filming, we trimmed each video into clips wherein the background was motionless.

Automated tracking and quantification of movement

We developed Python scripts to detect tardigrades and measure size, speed, and direction of travel (www.github.com/enwudz/gait). The outline of the tardigrade in each video frame was used to determine area, length, and width, and center of mass coordinates. By comparing coordinates across each frame, we determined speed and direction of travel. We defined a 'stop' as a period of 0.3 seconds when the tardigrade moved ≤ 0.03 body lengths. Similarly, a 'turn' occurred when a tardigrade changed direction by ≥ 28˚ during 0.3 seconds. These thresholds were determined by iteratively optimizing the scripts until they matched qualitative calls of stops and turns in pilot videos. Forward motion without stops and turns was defined as a sustained walking bout.

Step kinematics

Sustained walking bouts of 3 seconds or longer were used to collect timing of swings and stances for individual legs. For each tardigrade, we selected 1-3 sustained walking bouts to analyze a total of at least 10 seconds of walking. If multiple candidate bouts were available, we prioritized individual bouts of ~8 seconds, corresponding to the time it takes for a typical tardigrade to travel across the span of a video frame.

We developed Python scripts to record step and swing timing semi-automatedly for each video clip. For each leg, we stepped through a sustained walking bout frame by frame, and recorded step timing via specific keystrokes as the claw contacted or released contact with the surface of the agarose. From timing of steps and swings for each complete stride (foot down to foot down), our scripts calculate stance and swing duration, duty factor, step period, and swing-swing offset timing between pairs of legs. When combined with the path tracking data above, step and swing times were used to calculate stride length (distance in floor-fixed coordinates between two consecutive stance onsets), stride speed, and change in direction per stride.

Interleg coordination

During periods where step and swing data were recorded, we assigned a hexapod coordination pattern to each video frame according to the identities of the lateral (first through third leg pair) legs that were in swing phase (Mendes et al., 2013; Pfeffer et al., 2019; Tross et al., 2022). Periods with all lateral legs in stance phase were classified as 'stand', and periods with one lateral leg in swing phase were classified as 'pentapod.' We subdivided periods of tetrapod gait (two legs in swing phase) into three categories: (1) tetrapod canonical, when the two swinging legs were diagonally oriented (i.e. contralateral to each other in adjacent segments), (2) tetrapod gallop, when the two swinging legs were within the same body segment, and (3) tetrapod other, when the two swinging legs did not match the canonical or gallop pattern. Similarly, we subdivided periods of tripod gait into two categories: (1) tripod canonical, when the three swinging legs were diagonally oriented, contralaterally in adjacent segments, and (2) tripod other, when the three swinging legs did not match the canonical tripod pattern. Finally, we divided rear leg stepping patterns into three groups: (1) stand (both rear legs in contact with the substrate), (2) step (one leg in swing phase), and (3) hop (both legs in swing phase).

Isolation of wild *Ramazzottius* and 18S rDNA sequencing

Samples of moss and lichen were collected from trees on the Ithaca College campus, and soaked overnight in Poland Spring water. Candidate *Ramazzottius* individuals were identified via their characteristic claw morphology and striped color pattern. After videos were taken, *Ramazzottius* individuals were isolated for 18S rDNA sequencing. Identities of a subset of the lab *Hypsibius exemplaris* individuals and wild-caught *Ramazzottius* individuals were confirmed by sequencing of 18S ribosomal DNA and alignment via BLAST with nucleotide sequences in GenBank (https://www.ncbi.nlm.nih.gov/nucleotide/). Genomic DNA was prepared from tardigrades via the HotSHOT technique (Truett et al., 2000), and amplicons for all

sequenced individuals were obtained via Polymerase Chain Reactions using the following primers: F566: 5'-CAGCAGCCGCGGTAATTCC-3', R1200: 5'-CCCGTGTTGAGTCAAATTAAGC-3' (Hadziavdic et al., 2014). All lab tardigrade sequences (n=14) matched GenBank accession number MG800327 (*Hypsibius exemplaris* strain Sciento Z151) via BLAST.

Isolation of juvenile tardigrades

Hypsibius exemplaris adults deposit eggs in their discarded cuticle (exuvium) during molting. To isolate freshly-hatched juvenile tardigrades, we transferred individual egg-containing exuviae to empty agar-coated Petri dishes, and photographed each exuvium at the same time on each subsequent day. Walking tardigrades were prepared for video tracking as soon as they were found, thereby ensuring that fewer than 24 hours had elapsed after hatching. When possible, we would wait as juvenile tardigrades actively emerged from their exuvium, and film them immediately thereafter.

Disulfiram treatment

For each disulfiram experiment, we selected 20-24 large tardigrades with bright green-colored gut contents, and distributed them evenly between two Petri dishes coated with 2% agarose. We avoided tardigrades that appeared more brown rather than green, as these brown tardigrades typically contain large eggs and, when treated with disulfiram, often become trapped within their own exuviae after egg expulsion. We prepared 5 mL of control and 1.1 μM disulfiram solutions of Poland Spring water and 1% DMSO, and added these solutions to the two dishes. We added 5 drops of concentrated *Chloroccum* to each dish, and incubated the two dishes within a single box in the dark, overnight at room temperature. After 24 hours of incubation, we screened each dish for walking tardigrades, and prepared them for videography as above.

Statistics

Spearman's ρ was used to calculate correlations. Regression fit lines, histogram density distributions, and probability density functions were generated via the Python package seaborn (Waskom, 2021). Distributions for pair-wise comparisons were evaluated for normal distributions via the Shapiro-Wilk test, and Levene's test was conducted to assess equal variance. A t-test was used in pairwise comparisons of normally distributed data, while the Mann–Whitney rank sum test was used to compare data that was not normally distributed. To correct for multiple hypothesis testing, the False Discovery Rate was controlled at 5% via the Benjamini-Yekutieli procedure. Statistical tests were conducted in Python via the scipy.stats module (Virtanen et al.,

2020). To compare the amount of time spent in particular coordination patterns, proportions were transformed into log ratios via the center log ratio method in the Python composition_stats module.

Results

Quantification of locomotion

To quantify locomotor behavior and establish a baseline for comparisons across treatments, we recorded an average of 139 (138.61 ± 23.45, mean ± s.d.) seconds of continuous video for 103 *Hypsibius exemplaris* individuals (Fig. 1A, Movie S1). We trimmed individual videos into clips (97.26 ± 18.67 seconds) for analysis (Fig. 1B).

Our setup enabled tracking of unconstrained walking in tardigrades over extended distances (22.25 ± 7.02 body lengths, Fig. S1). Automated measurements of body size and location were recorded during each video frame, and changes in location were used to calculate speed, distance, and direction of motion (Fig. 1A, F, G). Mean tardigrade length (251.53 ± 32.25) was within the range described for *Hypsibius exemplaris* (112-293 μm) (Gąsiorek et al., 2018), and lengths were strongly correlated with widths (Fig. 1C, $\rho=0.91$; $p<0.001$). Speed was calculated in physical distance (μm s^{-1}) and normalized to length (body length s^{-1}). Normalized speeds below thresholds (Methods) were defined as 'stops', and direction changes above thresholds were defined as 'turns' (Fig. 1D, F, G). Stops were often followed by turns: tardigrades ceased walking, compressed posteriorly, and oriented toward a new direction (Fig. 1D).

Tardigrades spent an average of 89% (88.68 ± 10.93%) of time in sustained walking (without turns or stops, Fig. 1E), and moved an average of 0.23 (0.23 ± 0.08) body lengths per second (Fig. S1). Size was correlated with speed in absolute units (Fig. S2A, B), but not when speed was normalized to body length (Fig. 1H, S2C). Tardigrades with a high width:length ratio moved more slowly (Fig. 1I).

Step kinematics

To quantify leg movements (Fig. 2A), we measured stance and swing initiation during periods of sustained walking (Fig. 2B), and analyzed an average of 128 (127.8 ± 41.5) complete strides over 14 (14.4 ± 3.2) seconds per individual (Fig. S3, Table S2). Rear legs have distinct musculature, innervation, and body orientation (Gross and Mayer, 2019), so we considered the first three leg pairs ('lateral legs') separately (Fig. 2B), as in a previous analysis of tardigrade locomotion (Nirody et al., 2021). Rear legs showed differences in swing and stance duration and distance covered per step compared to lateral legs (Fig. 2C-E, 3), whereas these values were

similar within lateral legs (Fig. 3). We measured 9471 strides in lateral legs, and 3692 in rear legs.

Like other panarthropods, tardigrades increase speed by decreasing stance duration (Fig. 3A) (Hughes, 1952; Nirody, 2021; Nirody et al., 2021). Swing duration decreased slightly with increasing speed, and remained largely constant at higher speeds (Fig. 3B) (Nirody, 2021; Nirody et al., 2021). Stance and swing durations and variance were similar within the lateral legs, while rear legs showed shorter stance durations, longer swing durations, and higher variance in swing duration (Fig. 2C, 3A, B, S4).

We used stance and swing times to calculate duty factors (proportion of a stride in stance phase) and step periods (elapsed time between stance onsets) for each stride (Fig. 2D, E). As shown previously (Nirody et al., 2021), duty factors showed a moderate inverse correlation with speed for all legs ($\rho = -0.55$ for first leg pair, $\rho = -0.58$ for fourth leg pair, Fig. 3C). Rear legs showed differences in stance and swing timing, leading to lower duty factors compared to lateral legs (Fig. 2D, 3C), indicating distinct control of these parameters. Step period, however, was similar across all legs, especially at higher speeds (Fig. 3D).

Ipsilateral coordination

To quantify coordination between ipsilateral legs, we measured offsets between swing initiations of neighboring legs along each side of the body. These offsets are typically normalized to the step period of the first leg in a paired comparison, and expressed as phase offsets (ϕ_I) ranging from 0 to 1. Phase offsets and duty factors determine which sets of legs are simultaneously in swing phase, and specific combinations of swinging legs determine the **i**nterleg **c**oordination **p**attern (ICP, Fig. S5). For combinations of six legs (hexapod, e.g. the lateral legs of tardigrades), ICPs are grouped into pentapod (one swinging leg), tetrapod, and tripod patterns. Combinations with more than three swinging legs are rare, presumably because they are not stable (Wilson, 1966). In hexapods, $\phi_I = 1/3$ and $2/3$ lead to tetrapod ICPs, while $\phi_I = 0.5$ generates a tripod ICP (Fig. S6). In our dataset, ϕ_I showed a bimodal distribution, with a peak at 1/3, and a shoulder at 2/3 (Fig. 4A, D, S7A-D).

In a walking ICP (S6A-D), neighboring ipsilateral legs rarely swing simultaneously. This pattern can be modeled by two simple rules: (1) swing onsets are suppressed while a neighboring leg is in swing phase, and (2) the likelihood of swing onset increases at the stance onset of a neighboring leg (Cruse, 1990; Dürr et al., 2004; Hughes, 1952; Wilson, 1966). Similar to previous tardigrade leg coordination analyses (Nirody et al., 2021), this pattern of suppression and release is clearly evident in our dataset (Fig. S8A, B, F, G). Compared to the second leg pair, the swing initiation of the first leg pair is slightly delayed (Fig. S8G). This observation, combined with the slightly larger duty factor for anteriormost legs (Fig. 3C), may

suggest a 'leading role' for forelegs in locomotion, as suggested by experiments in *Drosophila* (Mendes et al., 2013). Furthermore, some leg swings were initiated before stance onset of neighboring posterior legs (Fig. S8F, G); in insects, these early swings typically occur at highest speeds or shortest step periods (Wilson, 1966)

For a tetrapod ICP, $\phi_I < 0.5$ generates an anterograde -- from posterior to anterior, or metachronal (Wilson, 1966) -- wave of swings, while $\phi_I > 0.5$ generates an apparent retrograde wave (Fig. S6A, B), which occurs when the step period is shorter than the complete metachronal cycle (Wilson, 1966). Because $\phi_I = 2/3$ was prominent in our dataset, we sought to determine whether these offsets represented transient events, or if tardigrades walked for extended periods with an apparent retrograde wave of swings. We collected strides of third pair legs where ϕ_I was close to 2/3 (n=277), and plotted ϕ_I for the next step of that leg. The peak of the distribution was just below 2/3, suggesting that extended bouts of walking at $\phi_I = 2/3$ were common (Fig. S7F). These sustained $\phi_I = 2/3$ bouts would predict that a metachronal lag of 4/3 (2/3 + 2/3) would be evident in the dataset. The metachronal lag distribution (n=2793 strides for third pair legs) shows a strong peak at the canonical value of 2/3 ($\phi_I = 1/3$), and a shoulder at 4/3, again suggesting some sustained walking at $\phi_I = 2/3$ (Fig. S7G).

To quantify symmetry of ipsilateral leg coordination, we measured the metachronal lag on each side and calculated the absolute value of the $\log_2$ ratio (0 indicates complete symmetry). Over the ~14 seconds analyzed per tardigrade, the average absolute value of this $\log_2$ ratio was 0.34 (0.34 ± 0.25), indicating a difference of about 27% in metachronal lag between the two sides of the body. This asymmetry could potentially be generated by turns or by stochastic differences in coordination. To test whether a difference in metachronal lag was associated with turning, we plotted the change in direction in each step of the left third pair leg against the $\log_2$ ratio of (left metachronal lag/right metachronal lag) (n=1299 strides) and found that longer metachronal lag on the left (i.e. $\log_2(L3/R3) > 0$) was weakly correlated with turning to the left ($\rho = -0.13$, $p < 0.001$, Fig. S7H).

Contralateral coordination

To assess coordination between contralateral leg pairs, we calculated the contralateral phase offset (ϕ_C) by comparing swing onsets within each body segment. For tetrapod ICPs, ϕ_C = 1/3 or 2/3 result in simultaneous (synchronous) swing onsets and offsets for diagonally-oriented leg pairs (Fig. S6A, B), whereas a $\phi_C = 0.5$ generates asynchronous swings between diagonally-oriented legs (Fig. S6C). In contrast, a $\phi_C = 0$ produces a 'galloping' gait, wherein legs within a body segment swing simultaneously. For all legs, ϕ_C was centered around 0.5, indicating predominantly antiphase movement within contralateral leg pairs (Fig. 4B, D). The distribution of ϕ_C of lateral legs was qualitatively broader than that of ϕ_I (Fig. 4A, B, S7E),

suggesting that contralateral coordination is more flexible than ipsilateral coordination, in agreement with previous analyses (Dürr et al., 2004; Nirody et al., 2021; Schilling and Cruse, 2020). Accordingly, coupling between leg movements is less pronounced for contralateral leg pairs than for ipsilateral pairs (Fig. S8A, F). In contrast to the lateral legs, ϕ_C for rear legs was tightly clustered at 0.5 (Fig. 4C), suggesting that anti-phase coordination is stronger in rear legs. Accordingly, coupling between swing duration and onset of contralateral leg swings is more pronounced for rear legs than lateral legs (Fig. S8D, E).

Interleg Coordination Patterns

Phase offsets and duty factors vary as animals alter speed or footfalls in response to environmental circumstances. Many animals have distinct, energetically optimal ICPs at different speeds, for example, from walking to trotting to galloping in quadrupeds (Alexander, 2006; Hoyt and Taylor, 1981; Struble and Gibb, 2022). In these animals, transitions between gaits are marked by abrupt shifts in phase offsets and/or duty factors. In contrast, panarthopods like *Drosophila* and tardigrades show gradual changes in duty factor and phase offsets as speed changes (Nirody, 2021; Nirody et al., 2021; Wosnitza et al., 2012). For example, *Drosophila* adults primarily utilize a pentapodal ICP while moving slowly, and gradually shift to tetrapodal and tripodal ICPs with increased speed (Mendes et al., 2013; Nirody, 2021; Wosnitza et al., 2012). In addition, insects show more variation in ICPs at low speeds (Kozacik, 1981; Wosnitza et al., 2012).

Lateral legs of tardigrades exhibit ICPs similar to those of hexapod animals like *Drosophila* or stick insects (Nirody et al., 2021). We assigned a hexapod ICP for every video frame, by determining which lateral legs were in swing phase (Fig. 2B, S5) (Pfeffer et al., 2019; Tross et al., 2022). Tetrapod patterns were most common (48%, with 37.5% as canonical tetrapod), followed by pentapod (35.8%), and tripod (8.3%, with 2.9% as canonical tripod) patterns (Fig. 4F, 5D, Table S3). Nirody and colleagues (Nirody et al., 2021) reported that on softer substrates, tardigrades occasionally walked with a 'galloping' gait, where legs within a segment swing simultaneously. To quantify similar behaviors, we subdivided tetrapod patterns into canonical tetrapod (with two diagonally-oriented swinging legs), tetrapod gallop, and other (any other combination of two swinging legs). Similarly, we subdivided tripod patterns into canonical tripod (with three swinging legs oriented diagonally), and other (other combinations of three legs swinging). While the canonical tetrapod ICP predominated, most tardigrades also employed a galloping pattern (Fig. 4F, 5D, S9D), likely because duty factor and phase offsets vary across time for both sides of the tardigrade. We categorized rear leg ICPs separately, and found that steps were most common (75.8%), followed by stand (17.6%) and hop (6.5%, Fig. 4G, 5E, S9).

Sustained maintenance of a particular ICP requires that phase offsets and duty factors remain constant. Coordination for a particular pattern can be quantified via a coordination strength score (CSS): the ratio of time during which a set of legs maintains a particular pattern versus the elapsed time between first swing onset and the last stance onset of all legs involved in that pattern (Wosnitza et al., 2012). When CSS=1, all participating legs have simultaneous swing and stance onsets. We calculated CSS for canonical tetrapod and canonical tripod bouts for each tardigrade. Average per-individual tetrapod CSS was 0.41 (0.41 ± 0.05) and tripod CSS was 0.17 (0.17 ± 0.08), and these scores were not correlated with walking speed (Fig. 4H, S9). These values indicate that the legs involved in particular patterns were not well coordinated in their stance and swing onsets, and that individual tardigrades employ several coordination patterns within a single bout of walking (Fig. 2B). Together, our analysis of step kinematics and interleg coordination (Fig. S3, S9), established a baseline of within-species variation to enable comparisons between life stages, species, and experimental treatments.

Preferred walking speed and stepping patterns

Though tardigrades do not show abrupt transitions between ICPs at different speeds, we hypothesized that they may show speed-dependent preferences for certain ICPs. By combining step timing with per-frame body location, we plotted individual lateral leg step speeds (n=5175 strides, Fig. 5A). From discontinuities within this distribution, we partitioned steps into low speed (n=1550, < 0.23 body lengths s^{-1}), medium speed (n=1992, between 0.23 and 0.35 body lengths s^{-1}), and high speed steps (n=839, > 0.35 body lengths s^{-1}). Phase offsets showed different distributions in these partitions (Fig. 5B). At low speeds, ϕ_I showed local maxima at 1/3 and 2/3, leading to anterograde (ϕ_I = 1/3) and apparent retrograde (ϕ_I = 2/3) waves of leg swings within a tetrapod ICP (Fig. 5C). With increased speed, ϕ_I converged at 1/3, generating a prominently canonical tetrapod gait with an anterograde wave of swings (Fig. 5C). Distribution of ϕ_C was broad at low speeds, but converged around 1/2 as speed increased (Fig. 5B). These changing distributions of ϕ_I and ϕ_C suggest that at high speeds, a canonical tetrapod gait with asynchronous stepping is preferred, whereas a canonical tetrapod gait with synchronous stepping is also present at low speeds.

To determine how ICP composition changes with speed, we quantified the percentage of frames spent in each hexapod (Fig. 5D) and rear (Fig. 5E) ICP within each speed partition. At low speeds, a pentapod pattern was the predominant hexapod configuration, followed by canonical tetrapod. With increased speed, prevalence of pentapod patterns decreased, while tetrapod and tripod patterns increased (Fig. 5D). For rear legs, steps and hops became more prevalent as speed increased, whereas the stand pattern decreased (Fig. 5E).

Coordination between rear legs and lateral legs

Rear legs show distinct step kinematic parameters compared to lateral legs, perhaps reflecting differences in innervation, musculature, orientation of the legs with respect to the body, increased ipsilateral distance between rear and lateral legs, and a primarily grasping (rear) vs. walking (lateral) function (Fig. 2, 3) (Nirody et al., 2021). However, the step periods of rear legs and lateral legs are similar, especially at higher speeds (Fig. 3D), suggesting that rear legs participate in body-wide coordination of leg movements. To visualize these patterns, we calculated the percentage of video frames during which a particular leg was simultaneously in swing phase with each of the other seven legs, thereby defining the most common 'swing partners' (Fig. 6A). For lateral legs, swing partners were diagonally located, in canonical tetrapod and tripod patterns (Fig. S5). Swing partnerships between rear legs and lateral legs were more common than lateral leg-lateral leg partnerships, presumably because rear legs spend more time in swing phase. Notably, swing partnerships between third legs and diagonally-oriented rear legs were particularly strong, whereas swing partnerships between rear legs and ipsilateral third legs were weaker (Fig. 6A). These partnerships suggest that despite the unique characteristics of rear legs, coordination between rear legs and third pair legs is similar to the coordination within lateral legs. If this coordination occurs, swings of third legs should be suppressed during swings of ipsilateral rear legs, and this suppression should be released at stance onset of the ipsilateral rear leg. We compared rear leg swing and stance timing with the timing of swing initiation in all other legs (Fig. 6B, C, Fig. S10). Swings of third legs were tightly coupled to the swing durations and stance onsets of ipsilateral rear legs (Fig. 6B, C). Moreover, rear legs and diagonally-oriented third pair legs tended to swing simultaneously (Fig. S10). These data suggest that rear legs participated in body-wide coordination, despite their locally distinct step kinematic parameters.

Comparing locomotion between juveniles and adults

We quantified more than 50 parameters of locomotion for each tardigrade, including measurements of whole-animal movement, step kinematics, and interleg coordination (Fig. S1, S3, S9, Table S1, S2, S3). Many of these parameters are intercorrelated. To compare locomotion between treatments, we selected a subset of 21 of these measurements based on independence (e.g. include duty factor but exclude stance duration) or particular interest (e.g. include both absolute speed and body-length normalized speed). We ran pairwise comparisons for these measurements, and corrected for multiple comparisons at FDR < 0.05 via the Benjamini-Yekutieli procedure (Fig. 7).

To compare juvenile and adult locomotion, we isolated 21 juveniles within 24 hours of hatching, and compared their movement to our adult dataset (n=103) (Movie S2, Table S4).

While adult tardigrades were not precisely age matched, they were all ≥ 192 μm in length (192-326 μm, mean 251 μm), and juveniles ranged from 124 to 150 μm (mean 137 μm, Fig. 7A). Juveniles moved at slower absolute speeds, but speeds were equivalent to adults when normalized to body length (Fig. 7A). These differences were reflected in parameters of step kinematics: juveniles took smaller steps with lateral legs in absolute distance (Fig. 7D), but larger steps when normalized to body length (Fig. 7E). In addition, stance and swing duration of rear legs was shorter in juveniles, indicating a decrease in step period and thus a higher turnover rate (Fig. 7A). Phase offsets during sustained walking were indistinguishable between adults and juveniles. Compared to adults, however, juveniles spent more time in a tripod canonical gait (Fig. 7F). Thus locomotion and coordination are similar between juveniles and adults, with juveniles spending more time in an ICP associated with higher speeds in hexapods.

Comparing locomotion between species

To document differences in locomotion between species, we compared *Hypsibius exemplaris* individuals (n=103) to tardigrades captured on the Ithaca College campus (Movie S3, Table S5). Captured tardigrades were grouped according to shared morphological characteristics (e.g. claw morphology and body pigmentation), and 24 tardigrades were classified as members of the *Ramazzottius* genus and selected for comparison. We sequenced a portion of 18S rDNA from nine of these individuals, and found that the best GenBank matches for all sequences were from *Ramazzottius*.

Ramazzottius individuals moved slower, and spent less time in sustained walking bouts (Fig. 7B, Table S5). Speed during walking bouts were similar, but direction of motion was more variable in *Ramazzottius* (Fig. 7C, G). Accordingly, while stance and swing durations were longer in *Ramazzottius,* these individuals traveled further per step (Fig. 7H, I). Remarkably, phase offsets and coordination patterns of lateral legs were indistinguishable between species, whereas the rear legs of *Ramazzottius* exhibited less time in 'step' mode and more time in 'stand' mode (Fig. 7J, K). Thus while whole-animal aspects of locomotion were quite different, lateral leg coordination during walking bouts was largely indistinguishable between species.

Drug treatment and locomotion

To disrupt locomotion via drug treatment, we selected disulfiram for its potential to broadly impact nervous system function (Movie S4, Table S6). Disulfiram inhibits a variety of metal-containing enzymes, including acetaldehyde dehydrogenase (Lanz et al., 2023), dopamine ß-hydroxylase (Musacchio et al., 1966), and tyramine ß-hydroxylase (Musacchio et al., 1964). Accordingly, disulfiram has been used to inhibit octopamine synthesis in *Drosophila* (Pyakurel et al., 2018). *Drosophila* mutants with disrupted octopamine synthesis show reduced

locomotor performance, including flight deficiencies and decreased walking speed (Brembs et al., 2007; Wosnitza et al., 2012). In humans, chronic disulfiram exposure has been associated with peripheral neuropathy and ataxia (Frisoni and Di Monda, 1989).

Disulfiram-treated tardigrades (n=34) were much slower than controls (n=33) overall, and during bouts of sustained walking (Fig. 7C, N). Accordingly, stance and swing durations were longer in disulfiram-treated individuals (Fig. 7C, L). During swing phase, disulfiram-treated tardigrades occasionally exhibited unusual movements: legs twirled or tapped before stance onset (Fig. 7O, Movie S5). To determine if increased swing durations after disulfiram treatment was due to decreased speed or from other differences during swing phase, we partitioned steps according to speed, and compared swing duration in each speed partition. Across all speeds, swing durations were longer in disulfiram-treated tardigrades (Fig. 7M). Thus disulfiram-treated tardigrades show decreased walking speed, increased stance and swing phase duration (and increased stride period), and unusual behaviors during swing phase. Even with these differences, phase offset timing and ICPs were indistinguishable from controls after disulfiram treatment (Fig. 7C, P).

Discussion

Automated tracking

In our tracking experiments, tardigrades roamed over large distances (average of 22 body lengths) and times (average of >90 seconds), facilitating extended collection of step kinematic and interleg coordination data (average of 16 strides for each of the 8 legs during sustained walking bouts). Location coordinates enabled quantification of speed and direction of travel during each video frame. This automated setup facilitates throughput, enabling a comprehensive picture of intraspecies variation and rapid screening for differences across treatments. Changes in step timing or interleg coordination underlying differences detected in initial screens can be uncovered by quantifying swing and stance onsets in the same videos.

Planar walking, as analyzed here and previously (Nirody et al., 2021; Shcherbakov et al., 2010), is likely uncommon in natural habitats of tardigrades. Our unconstrained system is compatible with future studies that include three-dimensional substrate features. Thus our system could be employed to analyze behaviors typical of more natural habitats, including klinokinetic behaviors, wherein animals vary rates of turning, depending on environmental features (Shcherbakov et al., 2010). One disadvantage of our setup is that measurements of footfall geometry, including step positioning, leg angles, and individual leg speeds (Mendes et al., 2013; Pfeffer et al., 2019) are difficult in an unconstrained environment.

Step kinematics and interleg coordination

Nirody and colleagues (Nirody et al., 2021) analyzed locomotion in 43 tardigrades on polyacrylamide gels (23 on high-stiffness and 20 on low-stiffness substrates). For the high-stiffness substrate, the focus of most of their analysis, they analyze 989 lateral leg strides and 382 rear leg strides, or ~60 complete strides per tardigrade. After optimization, we chose a single substrate stiffness (2% agarose), and recorded data for 103 tardigrades, with a total of 9471 lateral leg steps and 3692 rear leg steps, or ~128 complete strides per tardigrade.

For time-dependent step kinematic parameters (stance and swing duration, duty factor, step period), our measurements were between the high stiffness and low stiffness values found previously (Nirody et al., 2021), suggesting that tardigrades walk similarly on agarose and acrylamide. However, for distance-dependent parameters (e.g. body length, distance per step), our measurements were about 50-70% of those found in the previous study. The source of these discrepancies is not clear, but the sizes of the tardigrades in the previous study (body length mean=350 μm) were significantly larger than what we report (mean=251.5 μm). We verified tardigrade size via several independent measurements (Fig.1A), and our measurements are consistent with previous ranges for body length in *Hypsibius exemplaris* (mean=232 μm, range = 112-293 μm) (Gąsiorek et al., 2018), and with other studies that report body size in this species (Goldstein, 2022; Gross et al., 2019). In addition, we verified the taxonomic identity of these tardigrades by 18S rDNA sequencing.

Interleg coordination measurements were consistent with the previous study (Nirody et al., 2021). Tardigrades employed a canonical tetrapod coordination pattern 38% of the time (vs. 31% previously), and 3% of the time in a canonical tripod pattern (vs. 3%). We use a different method to quantify interleg coordination (Pfeffer et al., 2019; Tross et al., 2022), in which an ICP is assigned for each video frame, and are able to quantify a larger range of coordination patterns, including non canonical patterns like 'galloping'. This strategy allowed us to measure how closely tetrapod or tripod bouts conform to idealized coordination patterns, by calculating the coordination strength during each bout (Tross et al., 2022).

Changes in coordination patterns at different speeds

Panarthropods such as insects and tardigrades transition smoothly between stepping patterns as speed changes, and can employ several ICPs at a given speed (Bidaye et al., 2018; Mendes et al., 2013; Nirody et al., 2021). Although transitions between ICPs in these animals are smooth, there is evidence that the distribution of walking speed is not continuous. Rather, certain speeds are preferred, and these speeds are associated with characteristic stepping patterns. For example, walking speed in cockroaches clustered into two groups (Bender et al.,

2011), and specific walking speeds were underrepresented in a study of *Drosophila* gait (Mendes et al., 2013).

From discontinuities in the distribution of walking speeds, we subdivided steps into low, medium, and high speed partitions. At low speeds, the distribution of ϕ_I was bimodal, with a main peak at ϕ_I = 1/3 and a secondary peak of ϕ_I = 2/3, while the distribution of ϕ_C was broad (Fig. 5B). Intersections of ϕ_I and ϕ_C at 1/3 and 2/3 were prominent at low speeds, indicating tetrapod gait with synchronous stepping (Fig. 5E, S6A, B). These slow-moving tardigrades with bimodal ϕ_I were reminiscent of the tardigrades walking on a soft substrate in the study of Nirody et al. (Nirody et al., 2021). In their analysis, the prevalence of ϕ_I = 2/3 in these slower tardigrades was suggested to arise after occasional galloping steps where two legs within a segment swung simultaneously. After a gallop, one anterior leg would delay swinging to reset the tetrapod pattern (i.e. an anterior leg on one side would have ϕ_I = 1/3, while the delayed leg would have ϕ_I = 2/3). If this resetting behavior is prominent, most steps with ϕ_I = 2/3 (a delay to reset to the tetrapod pattern) would be followed by steps where ϕ_I = 1/3 (maintaining the tetrapod pattern). We tested this prediction by collecting steps in third pair legs where ϕ_I was close to 2/3, plotted ϕ_I for the subsequent step of that leg, and found evidence of sustained walking with ϕ_I = 2/3, rather than an immediate reset to ϕ_I = 1/3 (Fig. S7F). In addition, sustained ϕ_I = 2/3 for steps along one side of the body would produce a normalized metachronal lag of 4/3, which was prominent in our dataset (Fig. S7G). At faster speeds, the distribution of ϕ_I converged to 1/3, while the distribution of ϕ_C converged to 1/2, similar to previous observations of fast-moving tardigrades on a stiff substrate (Nirody et al., 2021). Prominent intersections of ϕ_I = 1/3 (or 2/3) and ϕ_C = 1/2 at fast speeds are consistent with tetrapod gait with asynchronous stepping (Fig. 5C, S6C).

Though multiple ICPs were present in each speed partition, representation of the different ICPs changed with increased speed (Fig 5D, E). Pentapod patterns were more prevalent at slower speeds, while tetrapod and tripod patterns became more prominent at faster speeds. Thus our dataset provides evidence for preferred walking speeds, with a mixture of ICPs within each speed, and speed-dependent preferences in step patterns (e.g. tetrapod with synchronous stepping at slow speeds, tetrapod with asynchronous stepping at fast speeds). Preferences for speed and step patterns may reflect optimal energetic economy or stability, or the possibility of distinct neural and motor programs at different speeds (Mendes et al., 2013).

Coordination between rear legs and lateral legs

Interestingly, despite the many distinct aspects of anatomy and step kinematics of rear legs, their step period is similar to that of lateral legs, especially at higher speeds (Fig. 3D). This similarity suggests that rear legs may participate in body-wide interleg coordination. Ipsilateral

fourth and third legs apparently followed the coordination rules that govern relationships between ipsilateral lateral legs (Cruse, 1990); third pair leg swings were suppressed when the ipsilateral rear leg was swinging, and this suppression was released upon stance onset of the rear leg (Fig. 6B, C, S10A,D). Accordingly, rear legs tended to swing simultaneously with contralateral third legs and ipsilateral second legs, creating a pattern similar to canonical tetrapod and tripod ICPs (Fig. 6A). Thus movement of rear legs is independent in terms of step kinematic parameters, yet intercoordinated with the rest of the legs.

Locomotion in juveniles

After embryonic stages, there is no apparent increase in cell number between juveniles and adults (Nelson et al., 2015). Juveniles are thus self-sufficient, miniature versions of adults (Gross et al., 2015). Accordingly, parameters of juvenile and adult walking were largely identical, and juveniles moved as rapidly as adults when speed was normalized to body length (Fig. 7A, D, E). However, juveniles appear to spend more time in a tripod ICP, a stepping pattern associated with faster speeds (Fig. 5D, 7F). This observation is similar to previous studies in stick insects, in which first instar nymphs primarily employ a tripod gait, whereas adults mostly walk in a tetrapod pattern (Graham, 1972). Graham (Graham, 1972) hypothesized that this difference resulted from size of the body relative to objects in the environment. Larger animals need to adjust their steps to navigate obstacles, and may need the additional stability from four legs contacting the ground. In contrast, smaller animals navigate around or over these obstacles.

Comparison between species

Compared to *Hypsibius exemplaris*, *Ramazzottius* individuals displayed slower overall speed, less sustained walking, more turns, and longer stance and swing durations (Fig. 7B, G-K). During bouts of sustained walking, the timing of interleg phase relationships was similar between species, as was time spent in canonical tetrapod and tripod stepping coordination patterns. Thus while high-level aspects of locomotion (speed, turns, stops, and starts) may differ, coordination between legs during walking bouts is conserved. These results are similar to those observed by Nirody and colleagues (Nirody et al., 2021), in which phase timing relationships between legs were similar despite significantly different speeds on substrates of different stiffnesses.

Disulfiram treatment

Disulfiram-treated tardigrades are slower, have fewer bouts of sustained walking, and have longer stance and swing durations. Despite these differences, interleg coordination is

unaffected in drug-treated tardigrades (Fig. 7C, P). While the mechanism by which disulfiram disrupts locomotion in tardigrades remains unknown, one possibility is that disulfiram disrupts octopamine synthesis by inhibiting tyramine ß-hydroxylase (Musacchio et al., 1964; Pyakurel et al., 2018). Importantly, tardigrades have a predicted 1:1 orthologous relationship (GenBank accession number OQV12655) via reciprocal BLAST with the *Drosophila* tyramine ß-hydroxylase protein sequence. *Drosophila* mutants lacking octopamine synthesis have deficiencies in locomotor performance (Brembs et al., 2007; Wosnitza et al., 2012), and octopamine modulates walking initiation in cockroaches (Gal and Libersat, 2010). Interestingly, octopamine appears to selectively regulate high-level aspects of locomotion in insects. For example, *Drosophila* lacking octopamine show deficiencies in flight initiation and maintenance, but have normal wingbeat frequencies and amplitudes during flying bouts (Brembs et al., 2007). Similarly, *Drosophila* lacking octopamine walk slower and less frequently, yet have normal step kinematics and interleg coordination during walking bouts (Wosnitza et al., 2012). Behaviors of disulfiram-treated tardigrades are consistent with these results, in which absence of octopamine causes defects in high-level control of movement (e.g. initiation and maintenance of locomotion), yet interleg coordination remains intact, suggesting that the processes that regulate these two aspects of movement are distinct.

Alternatively, the tapping and twirling motions observed in disulfiram-treated tardigrades, along with speed-independent increases in swing duration (Fig. 7M), suggest that sensory feedback or proprioception might be disrupted. *Drosophila* adults with inactivated sensory neurons in the legs show slower walking but intact interleg coordination (Mendes et al., 2013). In these sensory-deficient *Drosophila*, step precision and leg function was disrupted, leading to uncoordinated body and foot placement. These defects were especially apparent in slow-moving individuals; flies walking at fast speeds were less dependent on sensory feedback, suggesting movement at different speeds employs distinct locomotor mechanisms (Mendes et al., 2013). As in *Drosophila,* regulation of interleg coordination in tardigrades is apparently decoupled from neuronal programs that control initiation and maintenance of walking.

Tardigrades as a model for locomotion and movement disorders

Locomotion requires interactions between regions of the nervous system, nerves and muscles, and organisms and their environment. Computational analysis of locomotion facilitates integration of these distinct aspects of biology (Miller et al., 2012). Even with a relatively simple nervous system, patterns of limb coordination in tardigrades are conserved. The jointless motion of tardigrade legs may enable a more straightforward model of neuronal control of limb-based locomotion, compared to systems like insects where individual joints are controlled separately (Bidaye et al., 2018). Importantly, genes underlying many human movement disorders are

conserved in tardigrades (unpublished data). *Hypsibius exemplaris* individuals are transparent, which will facilitate functional studies using reporter genes, calcium indicators, and optogenetic analyses, and genetic toolkits are actively being developed in tardigrades (Goldstein, 2022). These tools, combined with the relatively small numbers of neurons in tardigrades, may help unlock the potential for cellular-level analyses of appendicular locomotion.

Acknowledgments

We thank the IC Tardigrade Tracks classes of 2021, 2022, and 2023 for methods development, drug treatment optimization, and capture of wild tardigrades, and Brooks Miner for discussions and advice.

Competing interests

No competing interests declared

Author Contributions

Conceptualization: TL, IW; Methodology: EA, CC, JR, KM, TL, IW; Software: IW; Investigation: EA, SH, KT, LA, VI, IW; Writing: IW; Editing: JR, VI, TL, IW; Funding Acquisition: TL, IW; Visualization: IW; Supervision: TL, IW.

Funding

National Science Foundation Louis Stokes Alliances for Minority Participation (award number 2110082)
William T. Grant Foundation (Grant ID #ODF-203161)
Ithaca College Collegiate Science and Technology Entry Program
Ithaca College Humanities and Sciences Summer Scholars Program

Figures

Figure 1

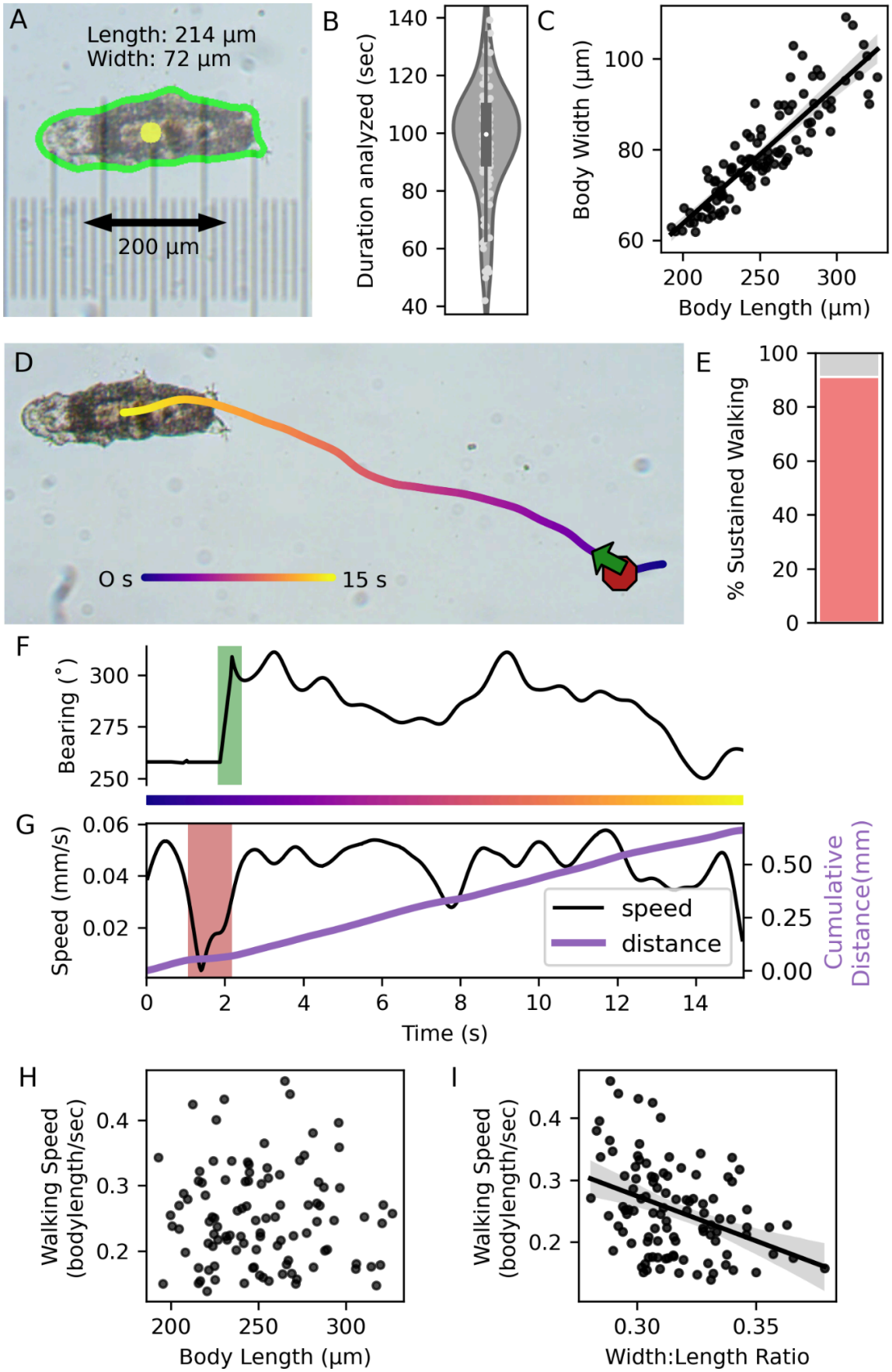
A
Length: 214 µm
Width: 72 µm
200 µm
B
Duration analyzed (sec)
140
120
100
80
60
40
C
Body Width (µm)
100
80
60
200
250
300
Body Length (µm)
D
O s
15 s
E
% Sustained Walking
100
80
60
40
20
0
F
Bearing (°)
300
275
250
G
Speed (mm/s)
0.06
0.04
0.02
Cumulative Distance(mm)
0.50
0.25
0.00
speed
distance
0
2
4
6
8
10
12
14
Time (s)
H
Walking Speed (bodylength/sec)
0.4
0.3
0.2
200
250
300
Body Length (µm)
I
Walking Speed (bodylength/sec)
0.4
0.3
0.2
0.30
0.35
Width:Length Ratio

Figure 1. Tracking and quantification of locomotion. A. Single video frame. Tardigrade outline (green) is automatically detected, and used to calculate length, width, and center of mass (yellow). A micrometer, at the same magnification and resolution, is superimposed to verify automated measurements. B. Video durations analyzed. C. Body width is strongly correlated to length ($\rho=0.905$, $p<0.001$). D. Image of the last frame of a ~15 second video, showing the tardigrade's path of motion, including a stop (red octagon) and a turn (green arrow). E. Proportion of sustained walking during the video from (D). F. Direction traveled during the video from (D); 0˚ = up, Green rectangle = turn. G. Speed and distance traveled during the video from (D). Red rectangle = stop. H. Normalized speed is not correlated with tardigrade length ($\rho = -0.003$, $p = 0.98$). I. Speed is inversely proportional to the width:length ratio ($\rho = -0.368$, $p < 0.001$). n=103 for panels B, C, H, I.

Figure 2

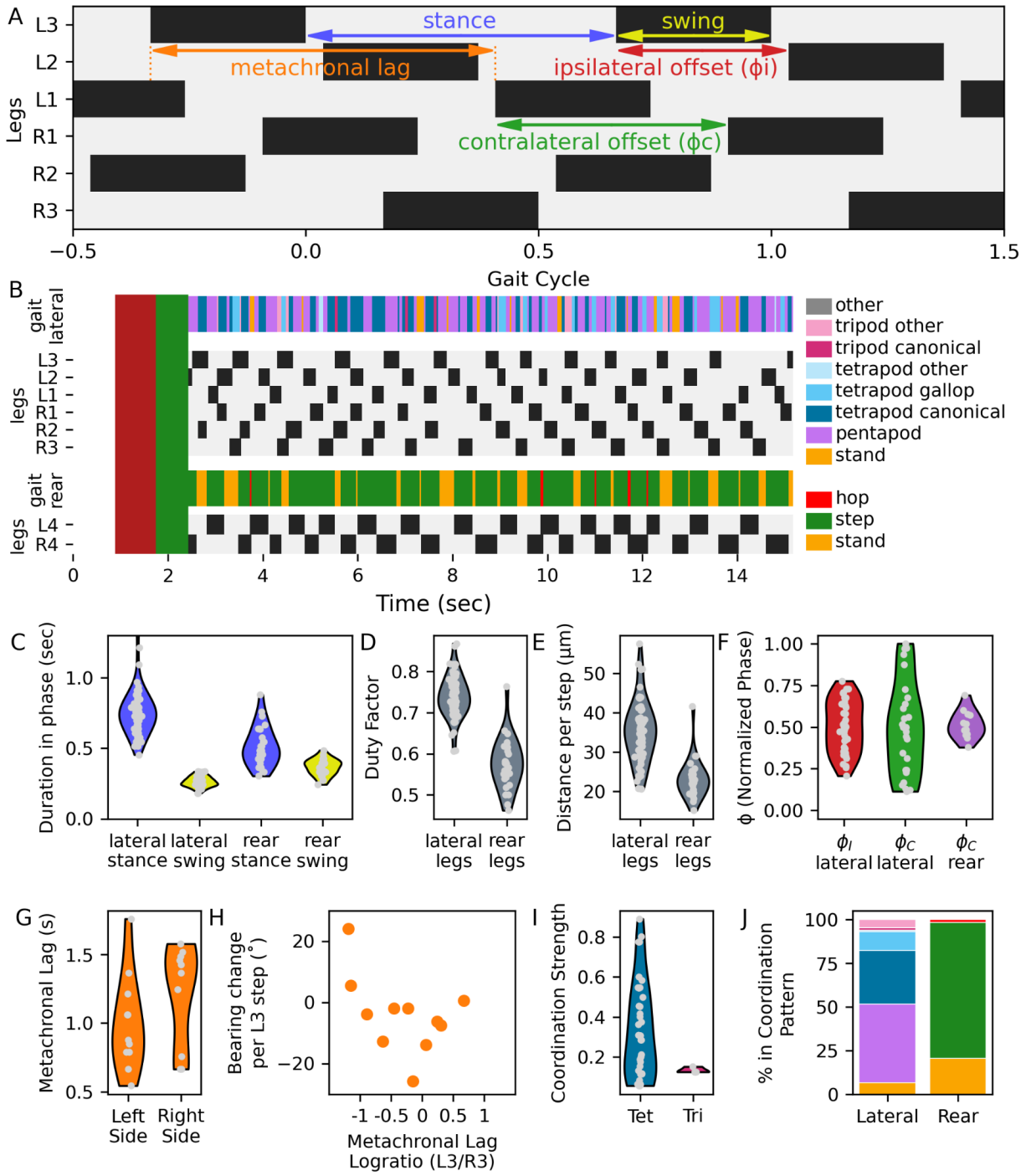
A
L3
L2
L1
R1
R2
R3
Legs
stance
swing
metachronal lag
ipsilateral offset (ϕi)
contralateral offset (ϕc)
−0.5
0.0
0.5
1.0
1.5
Gait Cycle
B
gait lateral
legs
L3
L2
L1
R1
R2
R3
gait rear
legs
L4
R4
other
tripod other
tripod canonical
tetrapod other
tetrapod gallop
tetrapod canonical
pentapod
stand
hop
step
stand
0
2
4
6
8
10
12
14
Time (sec)
C
Duration in phase (sec)
lateral stance
lateral swing
rear stance
rear swing
D
Duty Factor
lateral legs
rear legs
E
Distance per step (µm)
lateral legs
rear legs
F
ϕ (Normalized Phase)
ϕ_l lateral
ϕ_c lateral
ϕ_c rear
G
Metachronal Lag (s)
Left Side
Right Side
H
Bearing change per L3 step (°)
Metachronal Lag Logratio (L3/R3)
I
Coordination Strength
Tet
Tri
J
% in Coordination Pattern
Lateral
Rear

Figure 2. Step kinematics and interleg coordination. A. Example stepping pattern of lateral legs. Stance (gray) and swing (black) duration are recorded for each leg, and offset timing is calculated by comparing swing initiations between the neighboring ipsilateral anterior leg or the contralateral leg within a segment. Metachronal lag = elapsed time between swing onsets of a third leg and a first leg on one side, with an intervening swing in the second leg. B. Stance and swing timing and interleg coordination patterns (ICPs) for the video in Fig 1D. Red rectangle = stop; green = turn. Swing and stance onsets were recorded during periods of sustained walking. During each frame, the combination of legs in swing phase determined the ICP, with lateral legs (first three pairs, top) and rear legs (fourth pair, bottom) considered independently. L1 = anteriormost left leg; other legs are labeled similarly. C. Stance and swing duration for all steps. D. Duty factor -- the proportion of each stride spent in stance -- for all steps in this video. E. Distance per step. F. Phase offsets (ϕ_I = ipsilateral, ϕ_C = contralateral). G. Metachronal lag on the left vs. the right sides. H. Symmetry of metachronal lag plotted against change in direction for each step of the left third leg. I. Coordination strength scores for each canonical tetrapod or tripod ICP bout within this video. J. Percentage of the video spent in each ICP for lateral and rear legs. Color codes are as in (B).

Figure 3

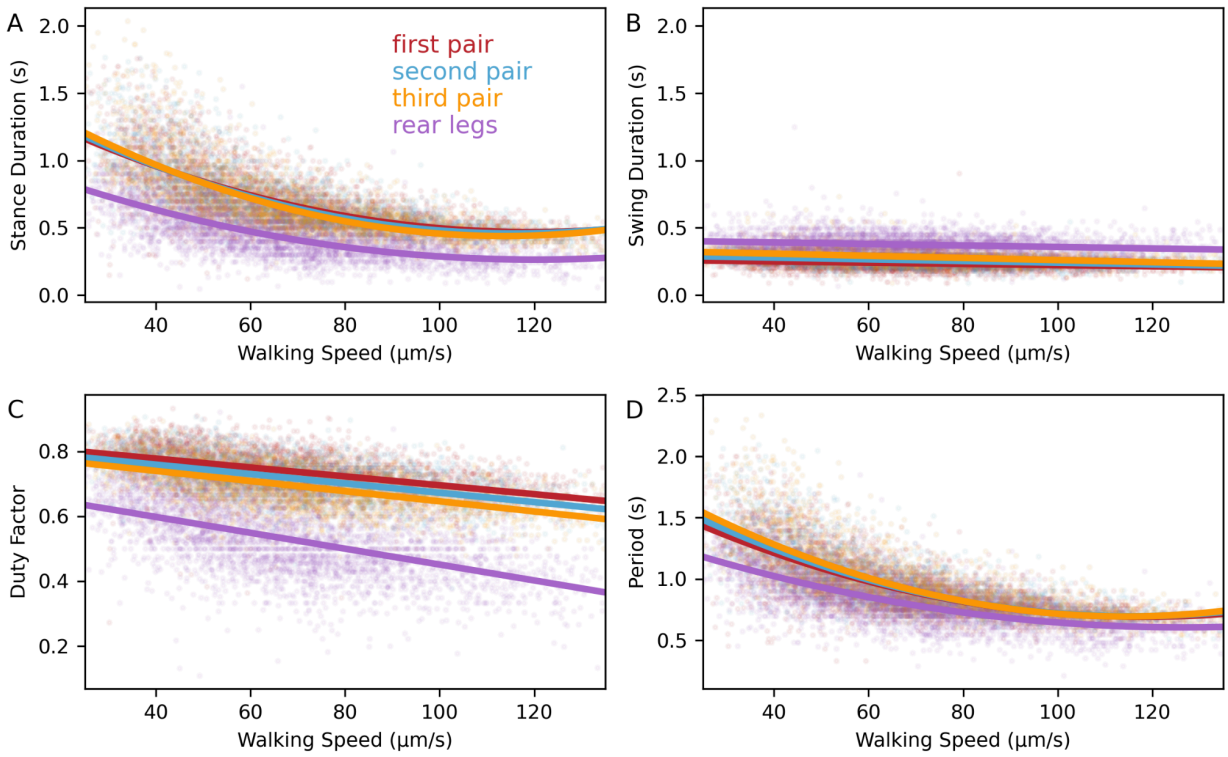

Figure 3. Speed and step kinematic parameters. A. Stance duration decreases with increased speed, and is lower in rear legs. B. Swing duration remains roughly constant with increasing speed, and is longer in rear legs. C. Duty factor decreases with increased speed. D. Step period decreases with increased speed. Color labels for all panels are as in (A). n=103 tardigrades, with 13163 total strides (first leg pair: 3221 strides, second: 3148 strides, third: 3102 strides, fourth: 3692 strides).

Figure 4

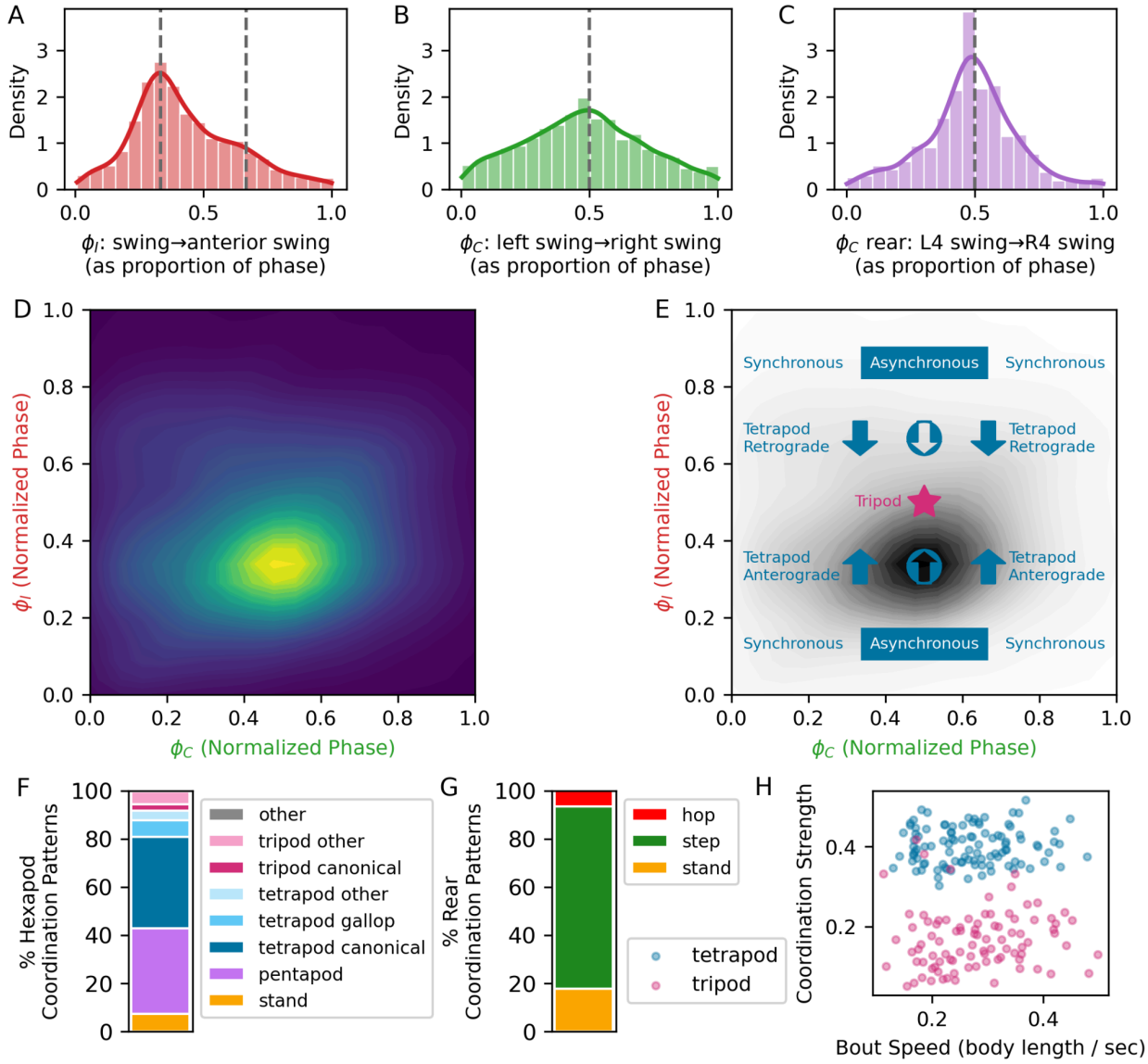
A
Density
ϕ_I: swing→anterior swing
(as proportion of phase)
B
ϕ_C: left swing→right swing
(as proportion of phase)
C
ϕ_C rear: L4 swing→R4 swing
(as proportion of phase)
D
ϕ_I (Normalized Phase)
ϕ_C (Normalized Phase)
E
Synchronous
Asynchronous
Synchronous
Tetrapod Retrograde
Tetrapod Retrograde
Tripod
Tetrapod Anterograde
Tetrapod Anterograde
Synchronous
Asynchronous
Synchronous
F
% Hexapod Coordination Patterns
other
tripod other
tripod canonical
tetrapod other
tetrapod gallop
tetrapod canonical
pentapod
stand
G
% Rear Coordination Patterns
hop
step
stand
tetrapod
tripod
H
Coordination Strength
Bout Speed (body length / sec)

Figure 4. Interleg phase offsets and coordination patterns. A. Distribution of ipsilateral phase offsets (ϕ_I): timing of swing initiation between lateral legs (in second or third pair) and the neighboring ipsilateral anterior leg (first or second pair), expressed as a fraction of the posterior leg step period. Dashed lines at 1/3 and 2/3 indicate offset values underlying canonical tetrapod gait, n=5175 strides. B. Distribution of contralateral phase offsets (ϕ_C): timing of swing initiation between left lateral legs and paired contralateral (right) legs, expressed as a fraction of the left leg step period, n=3809 strides. C. ϕ_C, rear: swing initiation timing between the left and right rear legs, expressed as a fraction of the left rear leg step period. n=1530 strides. D. Probability density plot of ϕ_C vs. ϕ_I for second and third pair legs, n=4414 strides. E. Diagram showing relationship between ϕ_I, ϕ_C, and canonical tetrapod or tripod coordination patterns, and observed distribution of ϕ_C vs. ϕ_I for for second and third pair legs. The highest density occurs at a canonical tetrapod pattern, with apparent anterograde wave of swings, and asynchronous swing initiations between the two legs participating in the pattern at each instant. F,G. Percentage of video frames spent in indicated hexapod (F) or rear leg (G) ICPs. H. Per-individual means of tetrapod and tripod bout speed vs. tetrapod and tripod coordination strength. n=103 tardigrades for all panels.

Figure 5

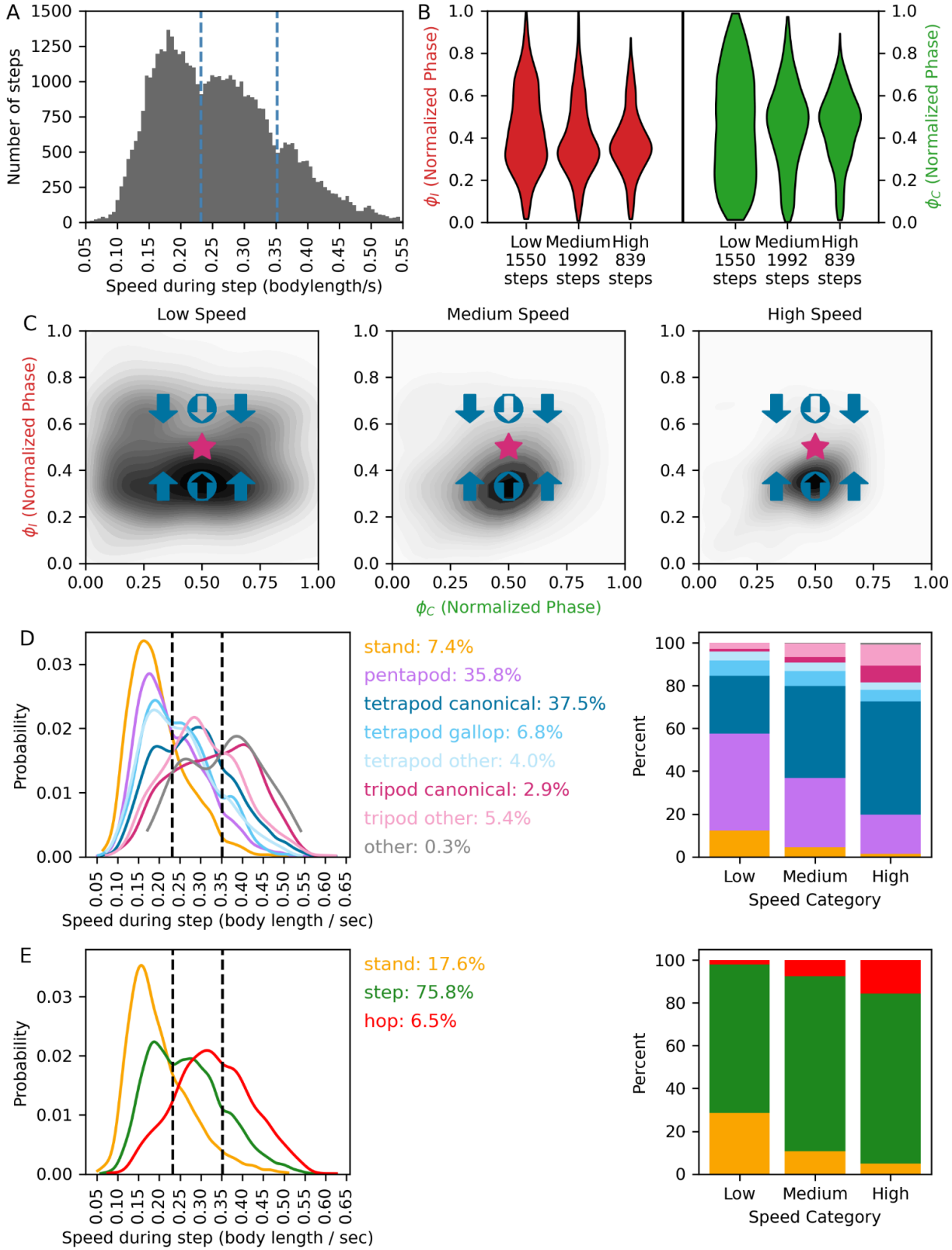
A
Number of steps
Speed during step (bodylength/s)
B
ϕ_I (Normalized Phase)
ϕ_C (Normalized Phase)
Low 1550 steps
Medium 1992 steps
High 839 steps
C
Low Speed
Medium Speed
High Speed
ϕ_I (Normalized Phase)
ϕ_C (Normalized Phase)
D
Probability
Speed during step (body length / sec)
stand: 7.4%
pentapod: 35.8%
tetrapod canonical: 37.5%
tetrapod gallop: 6.8%
tetrapod other: 4.0%
tripod canonical: 2.9%
tripod other: 5.4%
other: 0.3%
Percent
Low
Medium
High
Speed Category
E
Probability
Speed during step (body length / sec)
stand: 17.6%
step: 75.8%
hop: 6.5%
Percent
Low
Medium
High
Speed Category

Figure 5. Tardigrade preferences in walking speed and coordination patterns. A. Distribution of walking speed (bodylength s^{-1}) for 5175 steps of lateral legs. Walking speeds were subdivided into low, medium, and high partitions based on discontinuities in the distribution (dashed lines). B. Ipsilateral (ϕ_I) and contralateral (ϕ_C) phase offsets within speed partitions. C. Probability density plots of ϕ_C against ϕ_I in speed partitions, along with predicted stepping patterns at intersection points of ϕ_C and ϕ_I. D,E. Composition of hexapod ICPs for lateral legs (D), and rear ICPs (E). Left: Probability histograms of each individual stepping pattern at different speeds. Vertical lines show the speed partition boundaries in (A). Center: percentages indicate the proportion of all video frames wherein each particular coordination pattern is observed. Right: Changes in composition of each coordination pattern with increasing speed.

Figure 6

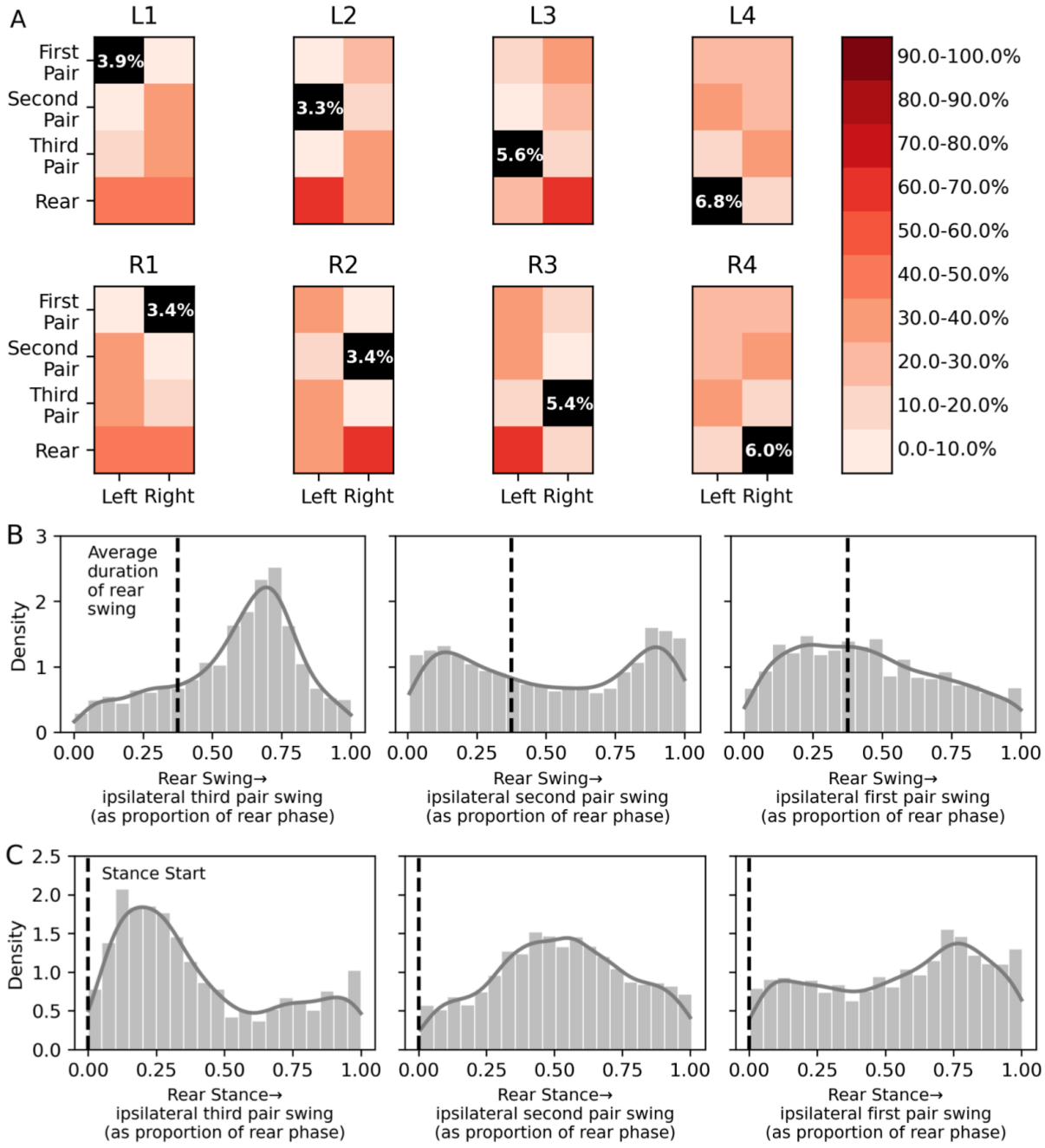
A
L1
L2
L3
L4
R1
R2
R3
R4
First Pair
Second Pair
Third Pair
Rear
3.9%
3.3%
5.6%
6.8%
3.4%
3.4%
5.4%
6.0%
Left Right
90.0-100.0%
80.0-90.0%
70.0-80.0%
60.0-70.0%
50.0-60.0%
40.0-50.0%
30.0-40.0%
20.0-30.0%
10.0-20.0%
0.0-10.0%
B
Average duration of rear swing
Density
Rear Swing→ ipsilateral third pair swing (as proportion of rear phase)
Rear Swing→ ipsilateral second pair swing (as proportion of rear phase)
Rear Swing→ ipsilateral first pair swing (as proportion of rear phase)
C
Stance Start
Density
Rear Stance→ ipsilateral third pair swing (as proportion of rear phase)
Rear Stance→ ipsilateral second pair swing (as proportion of rear phase)
Rear Stance→ ipsilateral first pair swing (as proportion of rear phase)

Figure 6. Coordination between rear legs and lateral legs. A. For the leg indicated on the top of each grid, colors within the grid show the percentage of video frames that each other leg is also in swing phase. Values in the black squares indicate the percentage of all frames during which that leg is the only leg swinging. B,C. Timing between swing duration (B) or stance initiation (C) of a rear leg and swing initiation in the ipsilateral third (left), second (middle), and first (right) legs, normalized to the step period of the rear leg. Average duration of rear leg swings (B) or stance onset timing (C) are shown by the dashed lines.

Figure 7

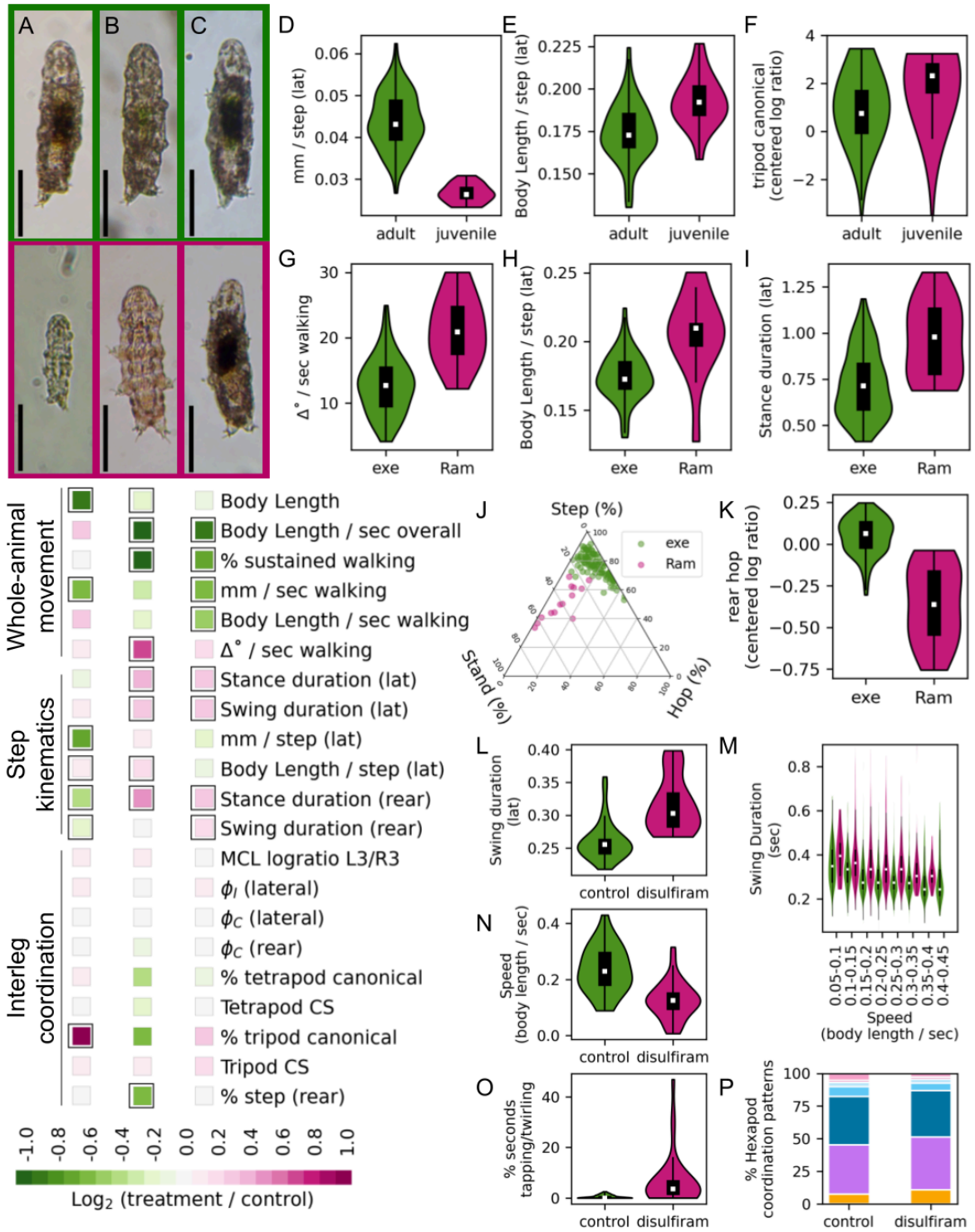
A
B
C
D
mm / step (lat)
adult
juvenile
E
Body Length / step (lat)
F
tripod canonical (centered log ratio)
G
Δ° / sec walking
exe
Ram
H
I
Stance duration (lat)
Whole-animal movement
Step kinematics
Interleg coordination
Body Length
Body Length / sec overall
% sustained walking
mm / sec walking
Body Length / sec walking
Δ° / sec walking
Stance duration (lat)
Swing duration (lat)
mm / step (lat)
Body Length / step (lat)
Stance duration (rear)
Swing duration (rear)
MCL logratio L3/R3
ϕ_l (lateral)
ϕ_C (lateral)
ϕ_C (rear)
% tetrapod canonical
Tetrapod CS
% tripod canonical
Tripod CS
% step (rear)
Log$_2$ (treatment / control)
J
Step (%)
Stand (%)
Hop (%)
K
rear hop (centered log ratio)
L
Swing duration (lat)
control
disulfiram
M
Swing Duration (sec)
Speed (body length / sec)
N
O
% seconds tapping/twirling
P
% Hexapod coordination patterns

Figure 7. Comparisons of walking across lifespan, species, and drug treatments. A-C. Representative images (top) and comparisons of locomotion (bottom) between the indicated pairs. exe = *H. exemplaris;* (Ram) = *Ramazzottius*. Colored squares show Log_2 (treatment / control) for each parameter, and black boxes indicate significance at FDR < 5% after correction for multiple comparisons. D-I Comparisons of indicated parameters. (D-E): adult vs. juvenile *H. exemplaris*; (G-I) adult *H. exemplaris* vs. *Ramazzottius* individuals. J-K Rear stepping pattern comparison (*H. exemplaris* vs. *Ramazzottius*). Compositional data underlying rear stepping patterns (J) were logratio transformed via the centered log ratio prior to comparison (K). L. Swing duration (control vs. disulfiram-treated tardigrades). M. Swing duration plotted against partitioned speed; swing durations of disulfiram-treated tardigrades were greater than controls for all speed partitions. N,O. Comparisons of the indicated parameters (control vs. disulfiram-treated tardigrades). P. Comparison of percentage of video frames spent in each hexapod ICP (control vs. disulfiram-treated tardigrades).

References

Alexander RM. 2006. Principles of animal locomotion, Princeton Paperbacks. Princeton: Princeton University Press.

Arakawa K, Yoshida Y, Tomita M. 2016. Genome sequencing of a single tardigrade Hypsibius dujardini individual. *Sci Data* **3**:160063. doi:10.1038/sdata.2016.63

Bender JA, Simpson EM, Tietz BR, Daltorio KA, Quinn RD, Ritzmann RE. 2011. Kinematic and behavioral evidence for a distinction between trotting and ambling gaits in the cockroach *Blaberus discoidalis*. *J Exp Biol* **214**:2057–2064. doi:10.1242/jeb.056481

Bidaye SS, Bockemühl T, Büschges A. 2018. Six-legged walking in insects: how CPGs, peripheral feedback, and descending signals generate coordinated and adaptive motor rhythms. *J Neurophysiol* **119**:459–475. doi:10.1152/jn.00658.2017

Brembs B, Christiansen F, Pflüger HJ, Duch C. 2007. Flight initiation and maintenance deficits in flies with genetically altered biogenic amine levels. *J Neurosci Off J Soc Neurosci* **27**:11122–11131. doi:10.1523/JNEUROSCI.2704-07.2007

Cruse H. 1990. What mechanisms coordinate leg movement in walking arthropods? *Trends Neurosci* **13**:15–21. doi:10.1016/0166-2236(90)90057-H

Dickinson MH, Farley CT, Full RJ, Koehl MAR, Kram R, Lehman S. 2000. How Animals Move: An Integrative View. *Science* **288**:100–106. doi:10.1126/science.288.5463.100

Dietz V. 1997. Neurophysiology of gait disorders: present and future applications. *Electroencephalogr Clin Neurophysiol* **103**:333–355. doi:10.1016/S0013-4694(97)00047-7

Dürr V, Schmitz J, Cruse H. 2004. Behaviour-based modelling of hexapod locomotion: linking biology and technical application. *Arthropod Struct Dev* **33**:237–250. doi:10.1016/j.asd.2004.05.004

Frisoni GB, Di Monda V. 1989. Disulfiram neuropathy: a review (1971-1988) and report of a case. *Alcohol Alcohol Oxf Oxfs* **24**:429–437.

Gal R, Libersat F. 2010. A Wasp Manipulates Neuronal Activity in the Sub-Esophageal Ganglion to Decrease the Drive for Walking in Its Cockroach Prey. *PLoS ONE* **5**:e10019. doi:10.1371/journal.pone.0010019

Gąsiorek P, Stec D, Morek W, Michalczyk Ł. 2018. An integrative redescription of Hypsibius dujardini (Doyère, 1840), the nominal taxon for Hypsibioidea (Tardigrada: Eutardigrada). *Zootaxa* **4415**. doi:10.11646/zootaxa.4415.1.2

Gibson ME, Stork N. 2021. Gait Disorders. *Prim Care Clin Off Pract* **48**:395–415. doi:10.1016/j.pop.2021.04.004

Giladi N, Horak FB, Hausdorff JM. 2013. Classification of gait disturbances: Distinguishing between continuous and episodic changes. *Mov Disord* **28**:1469–1473. doi:10.1002/mds.25672

Goldstein B. 2022. Tardigrades and their emergence as model organismsCurrent Topics in Developmental Biology. Elsevier. pp. 173–198. doi:10.1016/bs.ctdb.2021.12.008

Graham D. 1972. A behavioural analysis of the temporal organisation of walking movements in the 1st instar and adult stick insect (Carausius morosus). *J Comp Physiol* **81**:23–52. doi:10.1007/BF00693548

Gross V, Mayer G. 2019. Cellular morphology of leg musculature in the water bear *Hypsibius exemplaris* (Tardigrada) unravels serial homologies. *R Soc Open Sci* **6**:191159. doi:10.1098/rsos.191159

Gross V, Treffkorn S, Mayer G. 2015. Tardigrada In: Wanninger A, editor. Evolutionary Developmental Biology of Invertebrates 3. Vienna: Springer Vienna. pp. 35–52. doi:10.1007/978-3-7091-1865-8_3

Gross V, Treffkorn S, Reichelt J, Epple L, Lüter C, Mayer G. 2019. Miniaturization of tardigrades (water bears): Morphological and genomic perspectives. *Arthropod Struct Dev* **48**:12–19. doi:10.1016/j.asd.2018.11.006

Hadziavdic K, Lekang K, Lanzen A, Jonassen I, Thompson EM, Troedsson C. 2014. Characterization of the 18S rRNA Gene for Designing Universal Eukaryote Specific Primers. *PLoS ONE* **9**:e87624. doi:10.1371/journal.pone.0087624

Hoyt DF, Taylor CR. 1981. Gait and the energetics of locomotion in horses. *Nature* **292**:239–240. doi:10.1038/292239a0

Hughes GM. 1952. THE CO-ORDINATION OF INSECT MOVEMENTS.

Kozacik JJ. 1981. Stepping Patterns in the Cockroach, *Periplaneta Americana*. *J Exp Biol* **90**:357–360. doi:10.1242/jeb.90.1.357

Lanz J, Biniaz-Harris N, Kuvaldina M, Jain S, Lewis K, Fallon BA. 2023. Disulfiram: Mechanisms, Applications, and Challenges. *Antibiotics* **12**:524. doi:10.3390/antibiotics12030524

Mayer G, Kauschke S, Rüdiger J, Stevenson PA. 2013. Neural Markers Reveal a One-Segmented Head in Tardigrades (Water Bears). *PLoS ONE* **8**:e59090. doi:10.1371/journal.pone.0059090

Mendes CS, Bartos I, Akay T, Márka S, Mann RS. 2013. Quantification of gait parameters in freely walking wild type and sensory deprived Drosophila melanogaster. *eLife* **2**:e00231. doi:10.7554/eLife.00231

Miller LA, Goldman DI, Hedrick TL, Tytell ED, Wang ZJ, Yen J, Alben S. 2012. Using Computational and Mechanical Models to Study Animal Locomotion. *Integr Comp Biol* **52**:553–575. doi:10.1093/icb/ics115

Møbjerg N, Halberg KA, Jørgensen A, Persson D, Bjørn M, Ramløv H, Kristensen RM. 2011. Survival in extreme environments – on the current knowledge of adaptations in tardigrades. *Acta Physiol* **202**:409–420. doi:10.1111/j.1748-1716.2011.02252.x

Musacchio J, Kopin IJ, Snyder S. 1964. Effects of disulfiram on tissue norepinephrine content and subcellular distribution of dopamine, tyramine and their β-hydroxylated metabolites. *Life Sci* **3**:769–775. doi:10.1016/0024-3205(64)90032-3

Musacchio JM, Goldstein M, Anagnoste B, Poch G, Kopin IJ. 1966. Inhibition of dopamine-beta-hydroxylase by disulfiram in vivo. *J Pharmacol Exp Ther* **152**:56–61.

Nelson DR, Guidetti R, Rebecchi L. 2015. Phylum TardigradaThorp and Covich's Freshwater Invertebrates. Elsevier. pp. 347–380. doi:10.1016/B978-0-12-385026-3.00017-6

Nirody JA. 2021. Universal Features in Panarthropod Inter-Limb Coordination during Forward Walking. *Integr Comp Biol* **61**:710–722. doi:10.1093/icb/icab097

Nirody JA, Duran LA, Johnston D, Cohen DJ. 2021. Tardigrades exhibit robust interlimb coordination across walking speeds and terrains. *Proc Natl Acad Sci* **118**:e2107289118. doi:10.1073/pnas.2107289118

Pfeffer SE, Wahl VL, Wittlinger M, Wolf H. 2019. High-speed locomotion in the Saharan silver ant, *Cataglyphis bombycina*. *J Exp Biol* **222**:jeb198705. doi:10.1242/jeb.198705

Pirker W, Katzenschlager R. 2017. Gait disorders in adults and the elderly: A clinical guide. *Wien Klin Wochenschr* **129**:81–95. doi:10.1007/s00508-016-1096-4

Pyakurel P, Shin M, Venton BJ. 2018. Nicotinic acetylcholine receptor (nAChR) mediated dopamine release in larval Drosophila melanogaster. *Neurochem Int* **114**:33–41. doi:10.1016/j.neuint.2017.12.012

Schilling M, Cruse H. 2020. Decentralized control of insect walking: A simple neural network explains a wide range of behavioral and neurophysiological results. *PLOS Comput Biol* **16**:e1007804. doi:10.1371/journal.pcbi.1007804

Shcherbakov D, Schill RO, Brümmer F, Blum M. 2010. Movement behaviour and video tracking of Milnesium tardigradum Doyère, 1840 (Eutardigrada, Apochela). *Contrib Zool* **79**:33–38. doi:10.1163/18759866-07901002

Struble MK, Gibb AC. 2022. Do We All Walk the Walk? A Comparison of Walking Behaviors across Tetrapods. *Integr Comp Biol* **62**:1246–1280. doi:10.1093/icb/icac125

Tross J, Wolf H, Stemme T, Pfeffer SE. 2022. Locomotion in the pseudoscorpion *Chelifer cancroides* : forward, backward and upside-down walking in an eight-legged arthropod. *J Exp Biol* **225**:jeb243930. doi:10.1242/jeb.243930

Truett GE, Heeger P, Mynatt RL, Truett AA, Walker JA, Warman ML. 2000. Preparation of PCR-Quality Mouse Genomic DNA with Hot Sodium Hydroxide and Tris (HotSHOT). *BioTechniques* **29**:52–54. doi:10.2144/00291bm09

Virtanen P, Gommers R, Oliphant TE, Haberland M, Reddy T, Cournapeau D, Burovski E, Peterson P, Weckesser W, Bright J, Van Der Walt SJ, Brett M, Wilson J, Millman KJ, Mayorov N, Nelson ARJ, Jones E, Kern R, Larson E, Carey CJ, Polat İ, Feng Y, Moore EW, VanderPlas J, Laxalde D, Perktold J, Cimrman R, Henriksen I, Quintero EA, Harris CR, Archibald AM, Ribeiro AH, Pedregosa F, Van Mulbregt P, SciPy 1.0 Contributors, Vijaykumar A, Bardelli AP, Rothberg A, Hilboll A, Kloeckner A, Scopatz A, Lee A, Rokem A, Woods CN, Fulton C, Masson C, Häggström C, Fitzgerald C, Nicholson DA, Hagen DR, Pasechnik DV, Olivetti E, Martin E, Wieser E, Silva F, Lenders F, Wilhelm F, Young G, Price GA, Ingold G-L, Allen GE, Lee GR, Audren H, Probst I, Dietrich JP, Silterra J, Webber JT, Slavič J, Nothman J, Buchner J, Kulick J, Schönberger JL, De Miranda Cardoso JV, Reimer J, Harrington J, Rodríguez JLC, Nunez-Iglesias J, Kuczynski J, Tritz K, Thoma M, Newville M, Kümmerer M, Bolingbroke M, Tartre M, Pak M, Smith NJ, Nowaczyk N, Shebanov N, Pavlyk O, Brodtkorb PA, Lee P, McGibbon RT, Feldbauer R, Lewis S, Tygier S, Sievert S, Vigna S, Peterson S, More S, Pudlik T, Oshima T, Pingel TJ, Robitaille TP, Spura T, Jones TR, Cera T, Leslie T, Zito T, Krauss T, Upadhyay U, Halchenko YO, Vázquez-Baeza Y. 2020. SciPy 1.0: fundamental algorithms for scientific computing in Python. *Nat Methods* **17**:261–272. doi:10.1038/s41592-019-0686-2

Waskom M. 2021. seaborn: statistical data visualization. *J Open Source Softw* **6**:3021. doi:10.21105/joss.03021

Wilson DM. 1966. Insect Walking. *Annu Rev Entomol* **11**:103–122. doi:10.1146/annurev.en.11.010166.000535

Wilson RB, Keener AM. 2018. Movement Disorders in Children. *Adv Pediatr* **65**:229–240. doi:10.1016/j.yapd.2018.04.010

Wosnitza A, Bockemühl T, Dübbert M, Scholz H, Büschges A. 2012. Inter-leg coordination in the control of walking speed in *Drosophila*. *J Exp Biol* jeb.078139. doi:10.1242/jeb.078139

Supplementary Information

Supplemental Table S1

Supplemental Table S1. Measured parameters of whole-animal movement.

Measurement	Mean ± Std
Original Video Length (sec)	138.61 ± 23.45
Body Size (μm^2)	15081.68 ± 3753.68
Body Length (µm)	251.53 ± 32.25
Body Width (µm)	79.3 ± 11.1
Body Width/Length Ratio	0.32 ± 0.02
Distance traveled (mm)	5.55 ± 1.81
Body Lengths Traveled	22.25 ± 7.02
% sustained walking	88.68 ± 10.93
Speed (µm/sec)	58.97 ± 20.7
Speed (body lengths / sec)	0.23 ± 0.08
Speed (µm/sec walking)	63.28 ± 20.1
Speed (body lengths / sec walking)	0.25 ± 0.07
Bearing change (deg) / sec	16.34 ± 7.97
Bearing change (deg) / sec walking	12.62 ± 4.31
Stops / sec	0.09 ± 0.08
Turns / sec	0.05 ± 0.05
n=103 tardigrades	

Supplemental Table S2

Supplemental Table S2. Measured parameters of step kinematics.

Measurement	Mean ± Std
Steps Analyzed	127.8 ± 41.49
Seconds Analyzed	14.37 ± 3.21
Stance duration - lateral (sec)	0.72 ± 0.18
Stance duration - rear (sec)	0.47 ± 0.13
Swing duration - lateral (sec)	0.26 ± 0.03
Swing duration - rear (sec)	0.38 ± 0.05
Period - lateral (sec)	0.99 ± 0.2
Period - rear (sec)	0.85 ± 0.15
Duty factor - lateral	0.72 ± 0.04
Duty factor - rear	0.54 ± 0.07
Body Length / step lateral	0.17 ± 0.02
Body Length / step rear	0.11 ± 0.01
Metachronal lag (sec)	0.83 ± 0.26
Metachronal lag / Period	0.83 ± 0.14
Metachronal lag Log_2 Ratio	-0.01 ± 0.34
Abs Metachronal lag Log_2 Ratio	0.47 ± 0.2
Bearing Change ($^\circ$ s^{-1} step tracking)	6.32 ± 3.2
ϕ_I (lateral legs)	0.41 ± 0.07
ϕ_C (lateral legs)	0.49 ± 0.02
ϕ_C (rear legs)	0.5 ± 0.01
n=103 tardigrades	

Supplemental Table S3

Supplemental Table S3. Measured parameters of interleg coordination.

Measurement	Mean ± Std
% stand (lateral legs)	7.35 ± 5.25
% pentapod (lateral legs)	35.55 ± 10.66
% tetrapod canonical (lateral legs)	37.84 ± 12.13
% tetrapod gallop (lateral legs)	6.92 ± 4.39
% tetrapod other (lateral legs)	3.98 ± 2.32
% tetrapod total (lateral legs)	48.74 ± 10.91
% tripod canonical (lateral legs)	2.71 ± 3.47
% tripod other (lateral legs)	5.38 ± 4.04
% tripod total (lateral legs	8.1 ± 5.83
% stand (rear legs)	17.7 ± 10.73
% hop (rear legs)	6.55 ± 5.1
% step (rear legs)	75.75 ± 8.24
Tetrapod Coordination Strength	0.4 ± 0.05
Tripod Coordination Strength	0.17 ± 0.07
Tetrapod Bout Speed (bodylength s^{-1})	0.27 ± 0.08
Tripod Bout Speed (bodylength s^{-1})	0.28 ± 0.09
n=103 tardigrades	

Supplemental Table S4

Supplemental Table S4. Comparison of locomotion between adult and juvenile *H. exemplaris*.

	adult	juvenile	log2 ratio	Adjusted
Measurement	**mean ± s.d.**	**mean ± s.d.**	**juvenile/adult**	**p-value**
Body Length (mm)	0.25 ± 0.03	0.14 ± 0.01	-0.88	4.55E-11
Speed (body lengths s^{-1})	0.23 ± 0.08	0.28 ± 0.1	0.25	1.89E-01
Percentage of time cruising	88.68 ± 10.93	86.39 ± 24.21	-0.04	1.00E+00
Speed (mm/sec cruising)	0.06 ± 0.02	0.04 ± 0.01	-0.6	1.85E-04
Speed (body lengths s^{-1} cruising)	0.25 ± 0.07	0.3 ± 0.08	0.27	6.04E-02
Bearing change (deg) s^{-1} cruising	12.62 ± 4.31	13.4 ± 4.58	0.09	1.00E+00
Stance duration (lateral)	0.72 ± 0.18	0.67 ± 0.24	-0.11	3.01E-01
Swing duration (lateral)	0.26 ± 0.03	0.28 ± 0.03	0.08	2.37E-01
mm per step (lateral)	0.04 ± 0.01	0.03 ± 0.0	-0.72	1.07E-10
bodylength per step (lateral)	0.17 ± 0.02	0.19 ± 0.01	0.14	8.82E-04
Stance duration (rear)	0.47 ± 0.13	0.37 ± 0.15	-0.35	6.12E-03
Swing duration (rear)	0.38 ± 0.05	0.34 ± 0.04	-0.17	7.24E-03
Abs MCL Ratio per L3	0.47 ± 0.2	0.5 ± 0.26	0.1	1.00E+00
Anterior swing offsets (normalized, lateral)	0.41 ± 0.07	0.46 ± 0.07	0.14	1.46E-01
Opposite swing offsets (normalized, lateral)	0.49 ± 0.02	0.49 ± 0.02	0.01	1.00E+00
Opposite swing offsets (normalized, rear)	0.5 ± 0.01	0.49 ± 0.01	-0.01	2.36E-01
% tetrapod canonical (lateral)	37.84 ± 12.13	39.8 ± 10.5	0.07	1.00E+00
Tetrapod Coordination Strength	0.4 ± 0.05	0.4 ± 0.04	-0.01	1.00E+00
% tripod canonical (lateral)	2.71 ± 3.47	6.21 ± 4.46	1.19	1.15E-02
Tripod Coordination Strength	0.17 ± 0.07	0.17 ± 0.07	0.05	1.00E+00
% step (rear)	75.75 ± 8.24	76.43 ± 5.93	0.01	1.00E+00
n=103 adults, 21 juveniles				

Supplemental Table S5

Supplemental Table S5. Comparison of locomotion between adult and juvenile *H. exemplaris*.

	adult	juvenile	log2 ratio	Adjusted
Measurement	**mean ± s.d.**	**mean ± s.d.**	**juvenile/adult**	**p-value**
Body Length (mm)	0.25 ± 0.03	0.22 ± 0.03	-0.16	4.39E-03
Speed (body lengths s^{-1})	0.23 ± 0.08	0.12 ± 0.08	-0.97	5.12E-08
Percentage of time cruising	88.68 ± 10.93	39.72 ± 34.97	-1.16	2.64E-08
Speed (mm/sec cruising)	0.06 ± 0.02	0.05 ± 0.02	-0.34	1.32E-01
Speed (body lengths s^{-1} cruising)	0.25 ± 0.07	0.22 ± 0.06	-0.18	9.87E-01
Bearing change (deg) s^{-1} cruising	12.62 ± 4.31	21.19 ± 5.06	0.75	2.64E-08
Stance duration (lateral)	0.72 ± 0.18	0.97 ± 0.2	0.42	1.44E-04
Swing duration (lateral)	0.26 ± 0.03	0.32 ± 0.05	0.31	8.50E-04
mm per step (lateral)	0.04 ± 0.01	0.05 ± 0.01	0.05	1.00E+00
bodylength per step (lateral)	0.17 ± 0.02	0.21 ± 0.03	0.23	1.84E-04
Stance duration (rear)	0.47 ± 0.13	0.67 ± 0.25	0.52	3.52E-02
Swing duration (rear)	0.38 ± 0.05	0.38 ± 0.06	-0.01	1.00E+00
Abs MCL Ratio per L3	0.47 ± 0.2	0.49 ± 0.21	0.05	1.00E+00
Anterior swing offsets (normalized, lateral)	0.41 ± 0.07	0.42 ± 0.07	0.02	1.00E+00
Opposite swing offsets (normalized, lateral)	0.49 ± 0.02	0.49 ± 0.03	-0.01	1.00E+00
Opposite swing offsets (normalized, rear)	0.5 ± 0.01	0.47 ± 0.04	-0.08	5.67E-01
% tetrapod canonical (lateral)	37.84 ± 12.13	28.91 ± 10.23	-0.39	7.92E-02
Tetrapod Coordination Strength	0.4 ± 0.05	0.36 ± 0.06	-0.17	1.32E-01
% tripod canonical (lateral)	2.71 ± 3.47	1.77 ± 1.87	-0.62	1.00E+00
Tripod Coordination Strength	0.17 ± 0.07	0.18 ± 0.13	0.07	1.00E+00
% step (rear)	75.75 ± 8.24	51.08 ± 11.22	-0.57	3.97E-07
n=103 *Hypsibius exemplaris*, 24 *Ramazzottius*				

Supplemental Table S6

	adult	juvenile	log2 ratio	Adjusted
Measurement	**mean ± s.d.**	**mean ± s.d.**	**juvenile/adult**	**p-value**
Body Length (mm)	0.27 ± 0.03	0.25 ± 0.04	-0.12	1.02E-01
Speed (body lengths s^{-1})	0.24 ± 0.08	0.13 ± 0.07	-0.9	2.33E-05
Percentage of time cruising	87.7 ± 16.5	53.21 ± 30.61	-0.72	2.33E-05
Speed (mm/sec cruising)	0.07 ± 0.02	0.04 ± 0.01	-0.59	4.71E-04
Speed (body lengths s^{-1} cruising)	0.25 ± 0.08	0.18 ± 0.04	-0.49	9.96E-04
Bearing change (deg) s^{-1} cruising	11.96 ± 3.29	14.17 ± 5.29	0.24	5.44E-01
Stance duration (lateral)	0.75 ± 0.18	0.95 ± 0.18	0.35	7.46E-04
Swing duration (lateral)	0.26 ± 0.03	0.32 ± 0.04	0.28	3.95E-06
mm per step (lateral)	0.05 ± 0.01	0.04 ± 0.01	-0.18	1.41E-01
bodylength per step (lateral)	0.17 ± 0.02	0.16 ± 0.01	-0.08	1.67E-01
Stance duration (rear)	0.48 ± 0.11	0.57 ± 0.13	0.26	3.11E-02
Swing duration (rear)	0.38 ± 0.05	0.45 ± 0.08	0.23	6.31E-03
Abs MCL Ratio per L3	0.46 ± 0.2	0.45 ± 0.2	-0.04	1.00E+00
Anterior swing offsets (normalized, lateral)	0.44 ± 0.09	0.47 ± 0.12	0.09	1.00E+00
Opposite swing offsets (normalized, lateral)	0.48 ± 0.04	0.47 ± 0.05	-0.03	1.00E+00
Opposite swing offsets (normalized, rear)	0.49 ± 0.01	0.49 ± 0.02	-0.01	1.00E+00
% tetrapod canonical (lateral)	37.15 ± 11.67	35.39 ± 12.79	-0.07	1.00E+00
Tetrapod Coordination Strength	0.4 ± 0.05	0.41 ± 0.08	0.04	1.00E+00
% tripod canonical (lateral)	1.33 ± 1.66	1.61 ± 2.21	0.28	1.00E+00
Tripod Coordination Strength	0.15 ± 0.08	0.17 ± 0.11	0.21	1.00E+00
% step (rear)	76.07 ± 5.61	76.83 ± 7.32	0.01	1.00E+00
n=33 DMSO only, 34 disulfiram in DMSO				

Supplemental Figure S1

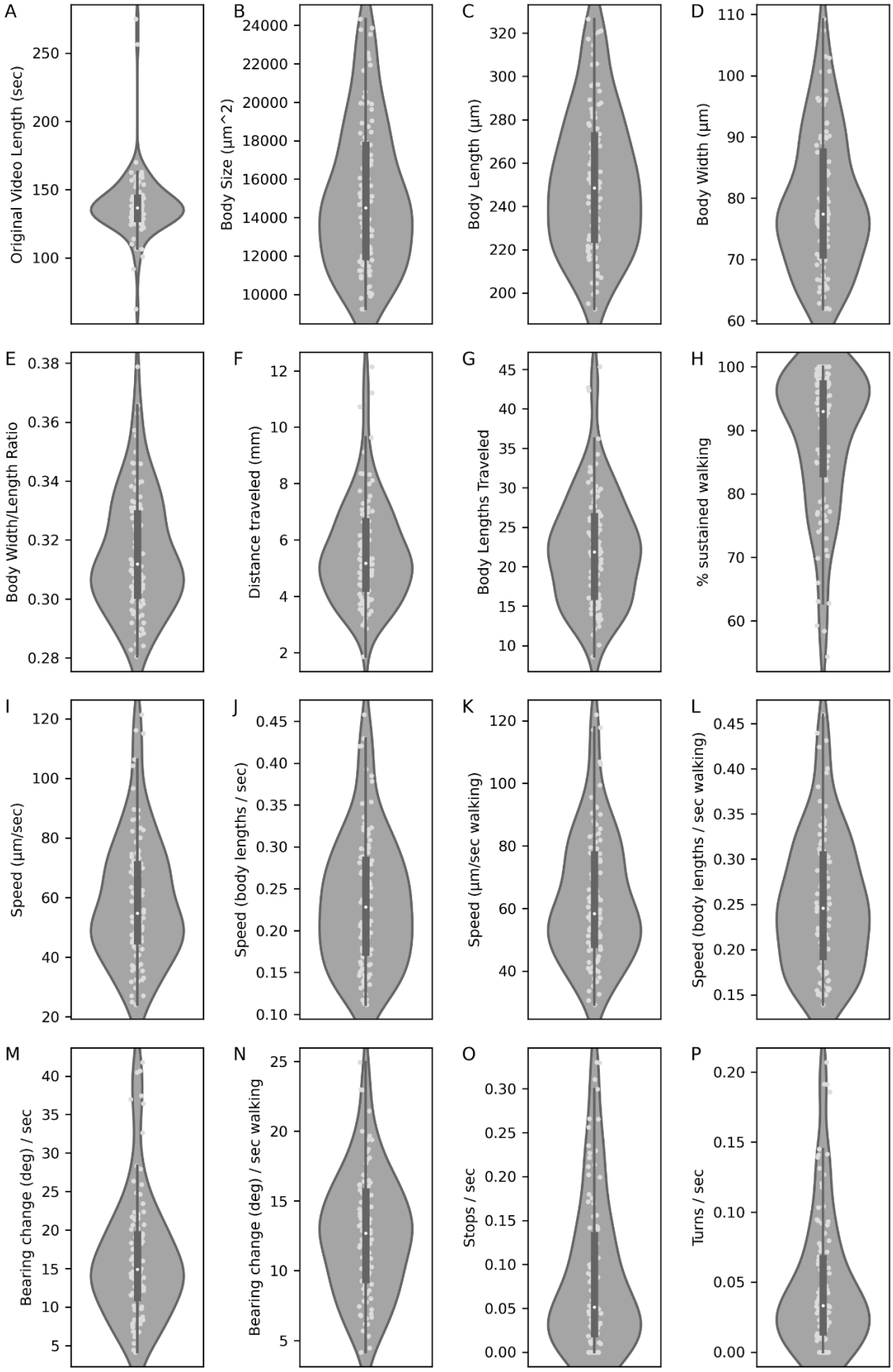

Supplemental Figure S1. Summary of whole-animal tracking values for 103 tardigrades. Each dot represents average data collected from an individual tardigrade.

Supplemental Figure S2

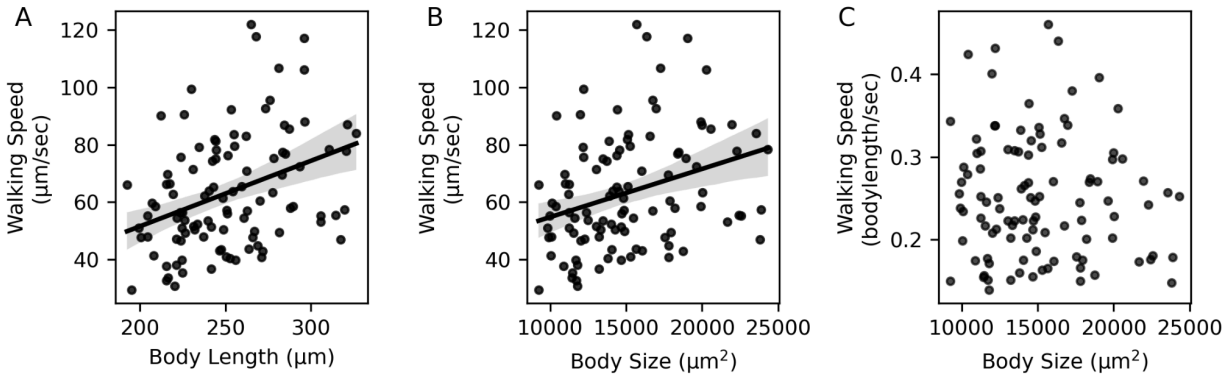

Supplemental Figure S2. Body size vs. speed. A. Walking speed is proportional to body length. B. Walking speed is proportional to body area. C. When normalized to body length, walking speed is not correlated with body size. Least squares regression fit lines and 95% confidence intervals were calculated in the Python package seaborn.

Supplemental Figure S3

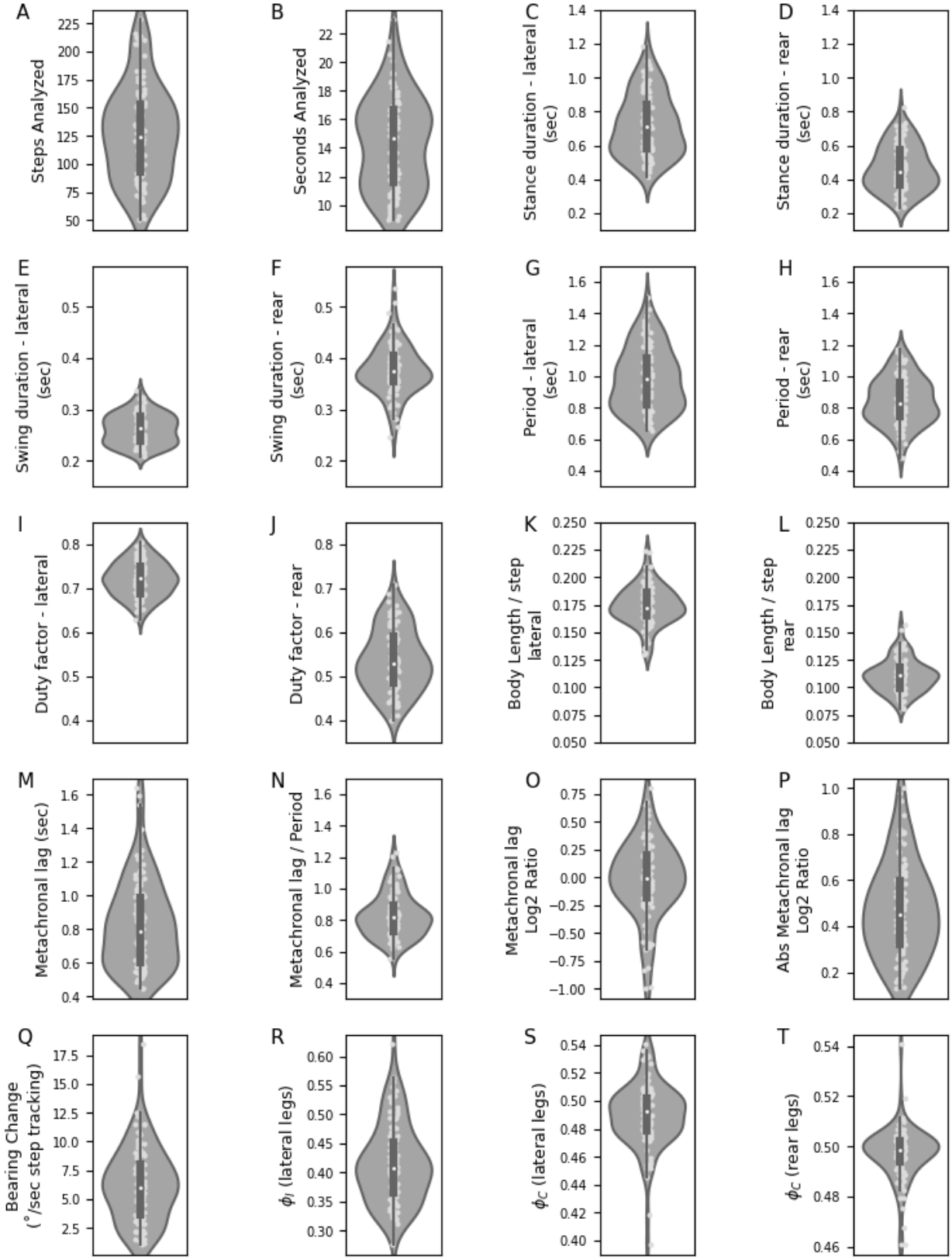

Supplemental Figure S3. Summary of step kinematics data for 103 tardigrades. Each dot represents average data collected from an individual tardigrade.

Supplemental Figure S4

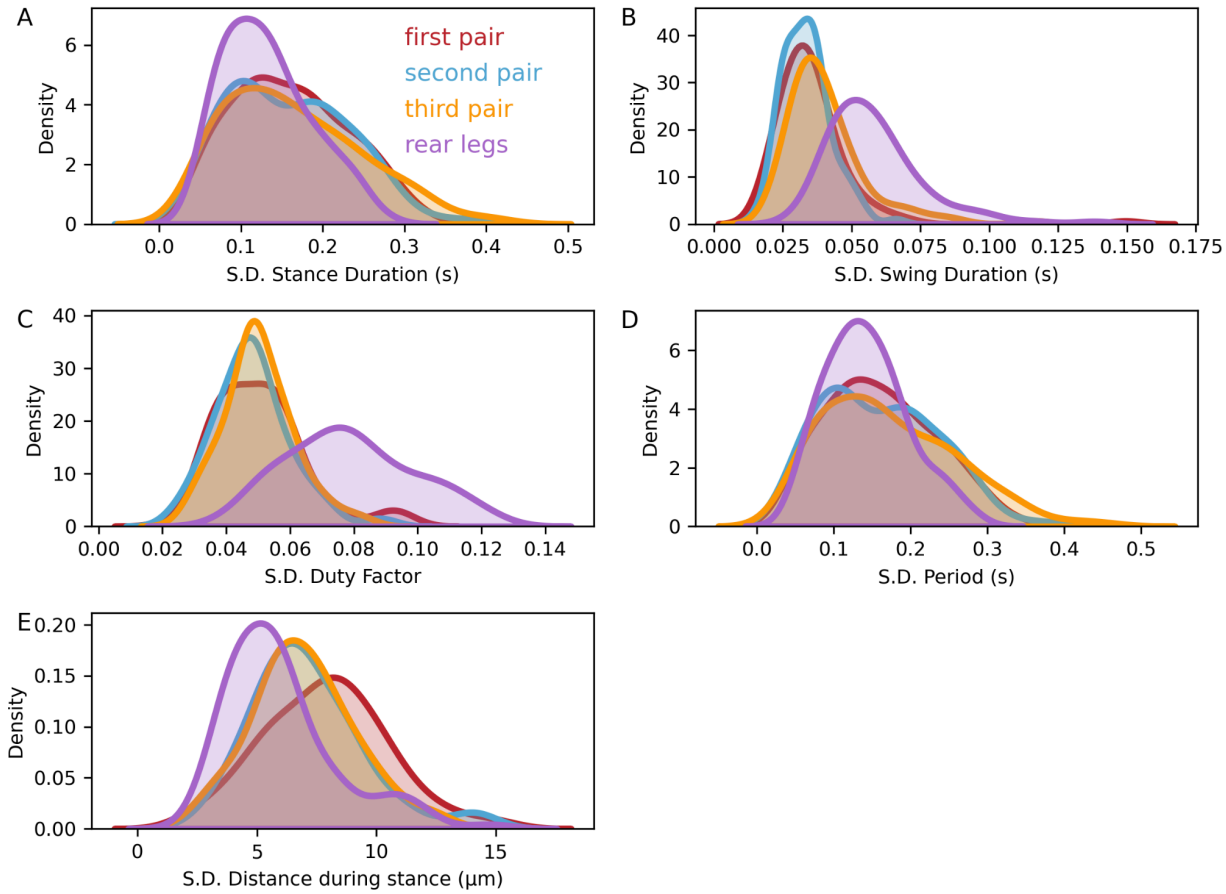

Supplemental Figure S4. Variance in step kinematics in each leg pair. Distributions of standard deviations for (A) stance durations, (B) swing durations, (C) duty factor, (D) step period, and (E) distance traveled per stance phase. Kernel density estimates of the distributions were calculated via the Python package seaborn. n=103 tardigrades.

Supplemental Figure S5

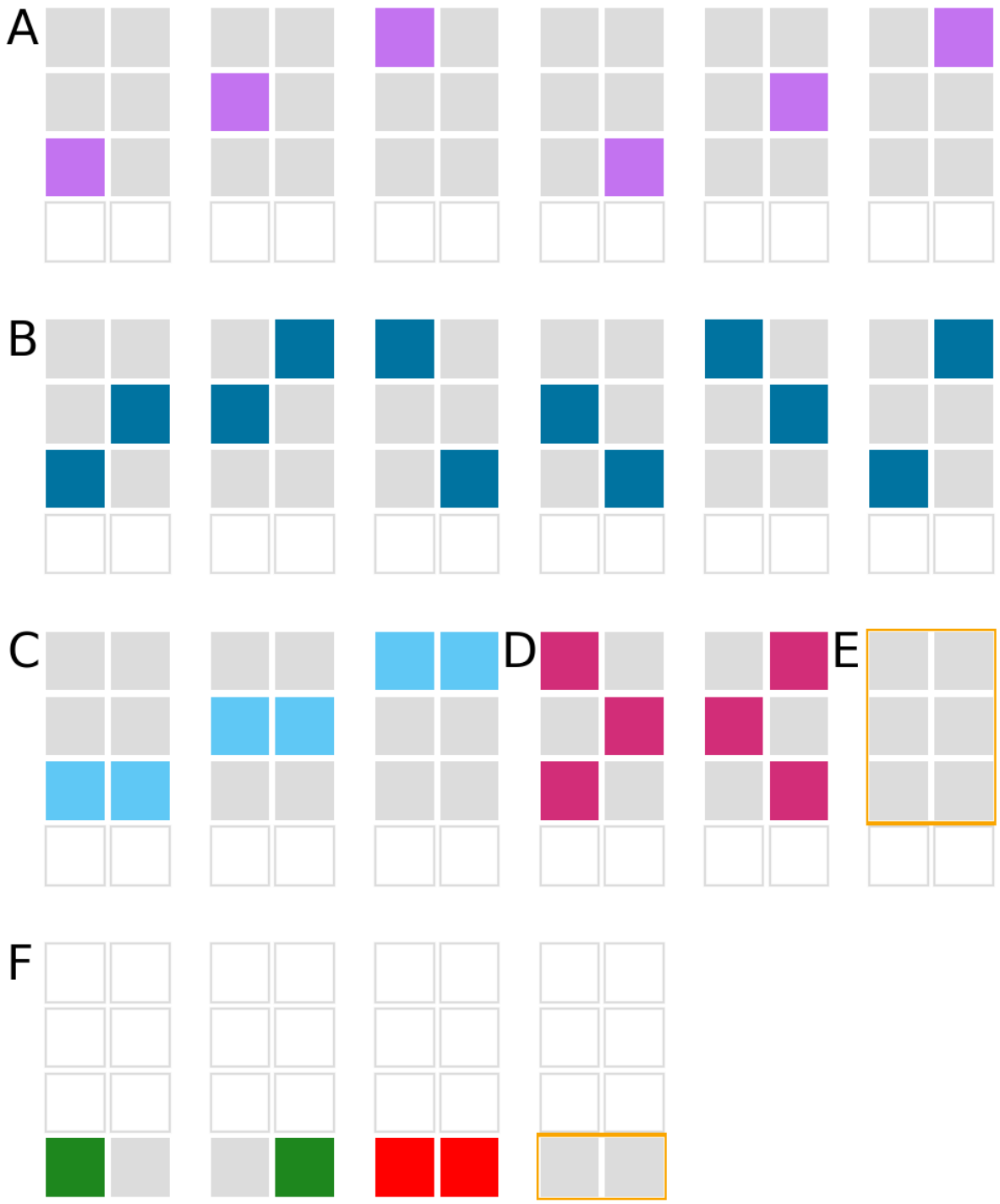

Supplemental Figure S5: Interleg coordination patterns. A-E Examples of hexapod interleg coordination patterns for lateral legs. A. Pentapod, B. Canonical Tetrapod, C. Tetrapod gallop, D. Tripod, E. Stand. F. Interleg coordination patterns for rear legs (stop, hop, stand).

Supplemental Figure S6

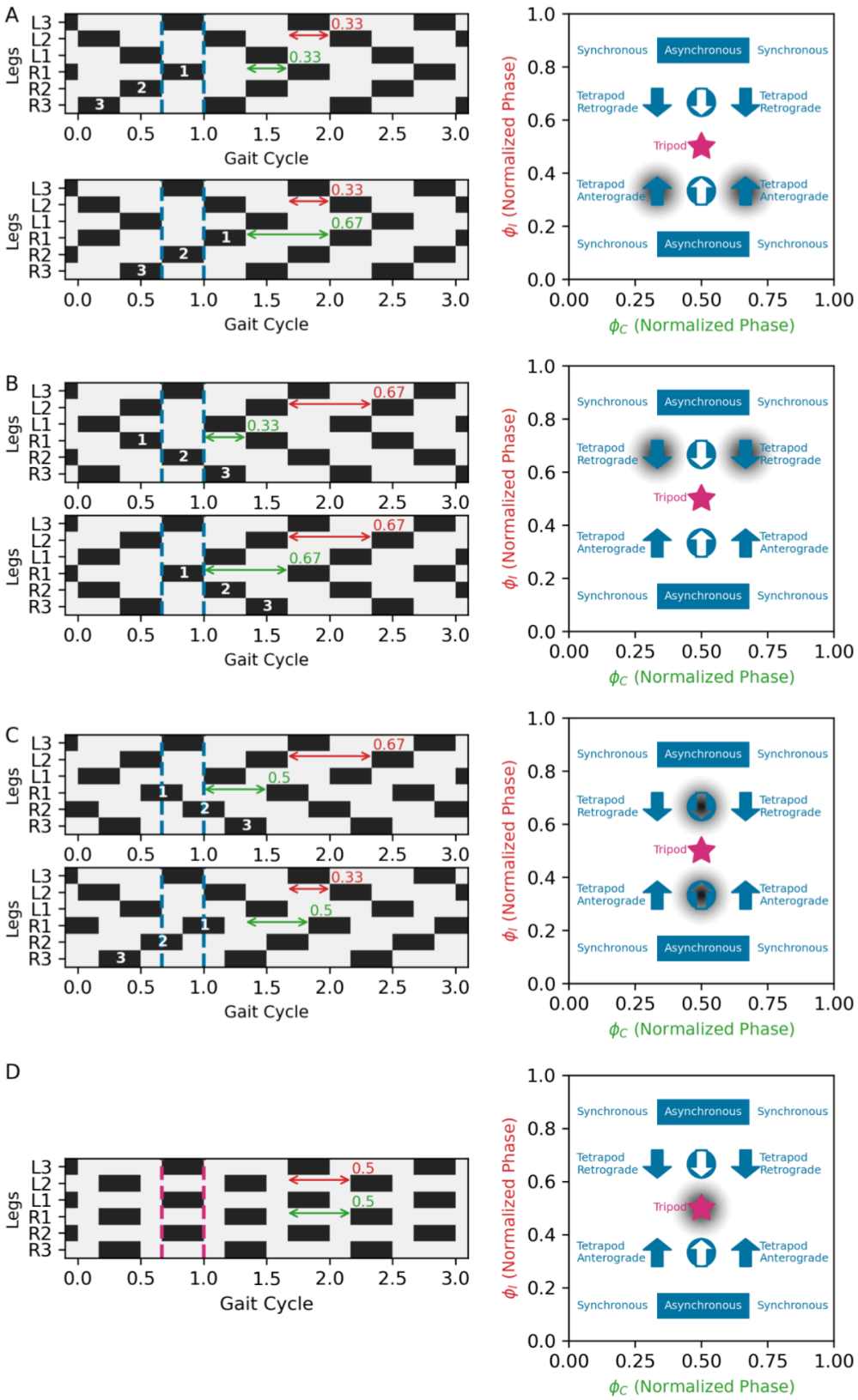

Supplemental Figure S6. Phase offsets determine hexapod stepping patterns. In all examples, duty factor for lateral legs is set at 2/3. A. When ϕ_I = 1/3 and ϕ_C = 1/3 or 2/3, a canonical tetrapod pattern is produced, with leg pairs initiating swing phase simultaneously (synchronous), and an anterograde (or metachronal) wave of swing initiations that travels from back to front. B. When ϕ_I = 2/3 and ϕ_C = 1/3 or 2/3, a canonical tetrapod pattern is produced, with leg pairs initiating swing phase simultaneously (synchronous), and an apparent retrograde wave of swing initiations that travels from front to back. C. When ϕ_I = 1/3 or 2/3 and ϕ_C = 1/2, a canonical tetrapod pattern is produced, with leg pairs initiating swing phase asynchronously. When ϕ_I = 1/3, the pattern of leg swings is anterograde, while when ϕ_I = 2/3, the swing initiation pattern is apparently reversed. When ϕ_I = 1/2 and ϕ_C = 1/2, a canonical tripod gait is produced.

Supplemental Figure S7

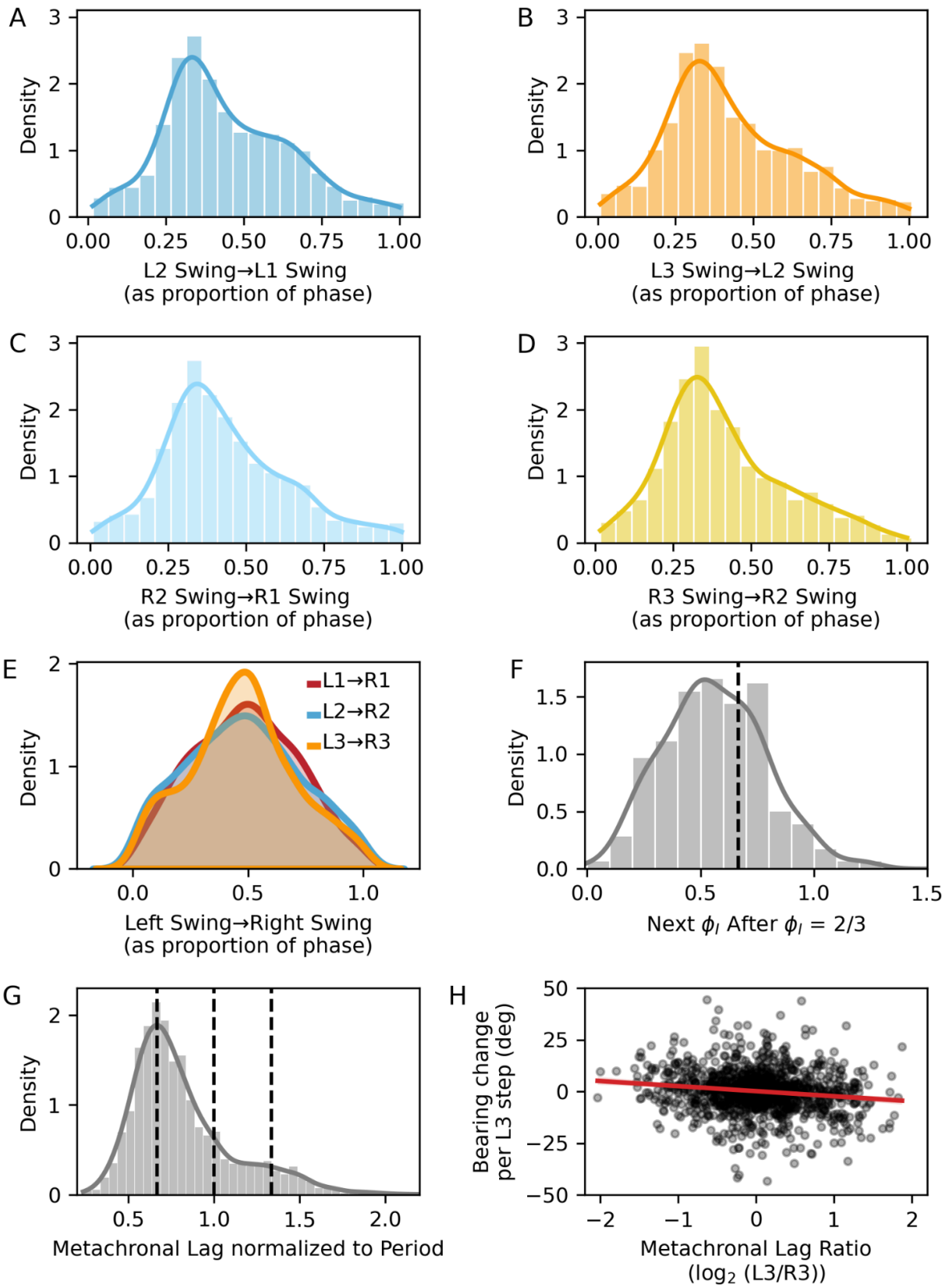

Supplemental Figure S7. Phase offsets and metachronal lag in individual legs. A-D. Distribution of ipsilateral phase offsets $(\phi)_i$ for each individual second or third pair leg. Timing of swing initiation between the indicated leg and the neighboring ipsilateral anterior leg, expressed as a fraction of the period of the posterior leg. n=1301 L2 steps for (A), 1279 L3 steps for (B), 1317 R2 steps for (C), 1278 R3 steps for (D). E. Distribution of contralateral phase offsets, or ϕ_C, for each left lateral leg. Timing of swing initiation between the indicated leg and the right leg within the same segment, expressed as a fraction of the period of the left leg. n=1305 steps for L1, 1251 steps for L2, 1253 steps for L3. F. Distribution of ϕ_i in third leg pair legs after a step after ϕ_i is about 2/3. The dashed line indicates $\phi_i = 2/3$. n=277 steps. G. Distribution of metachronal lag for all third pair legs. Dashed lines indicate values of 2/3, 1, and 4/3. n=2793 steps. H. Scatter plot of $\log_2$ ratio of metachronal lag of (left third pair leg (L3) / right third pair leg (R3)) plotted against direction change for each L3 step. Spearman $\rho = -0.13$, $p < 0.001$. n=1299 steps. Least squares regression fit line was generated via the Python package seaborn.

Supplemental Figure S8

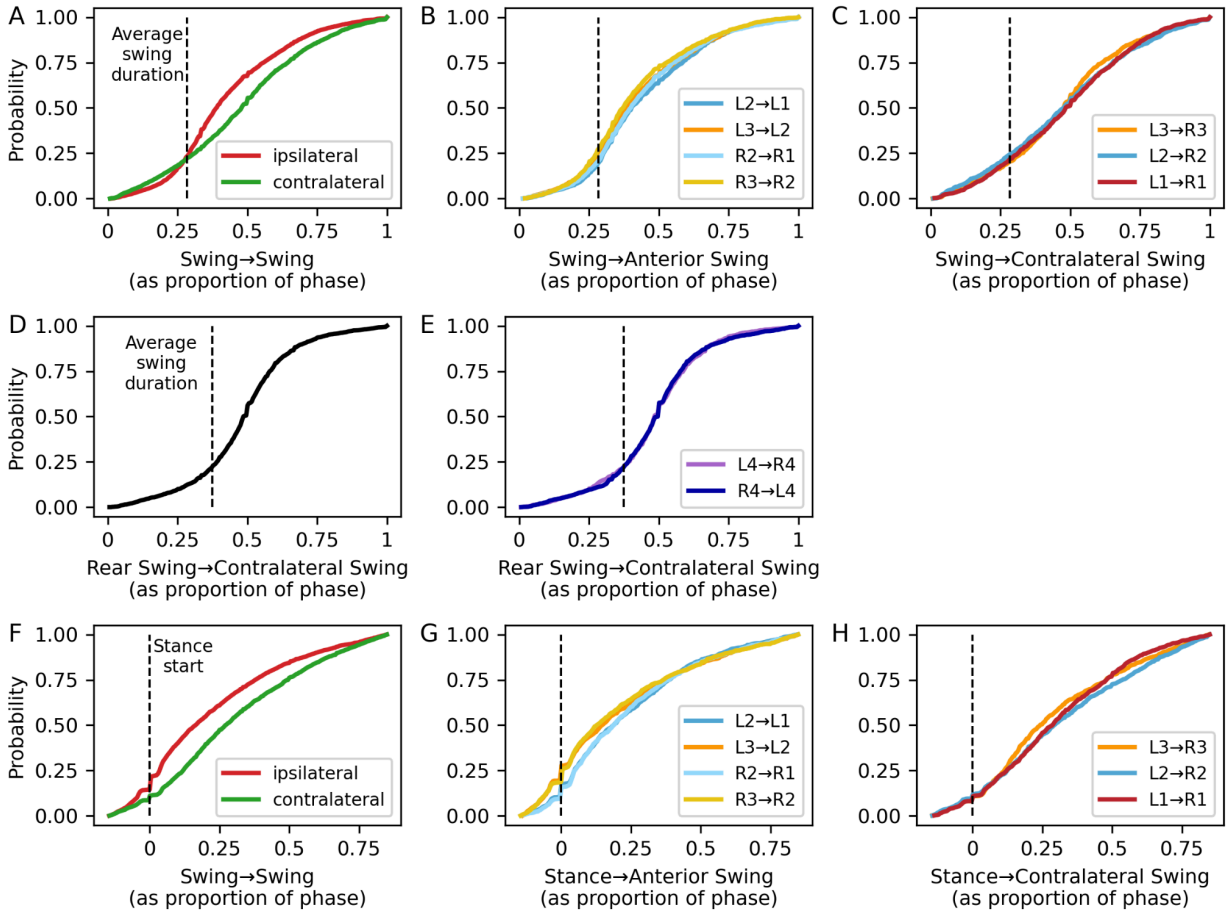

Figure S8. Suppression and initiation of neighboring leg swings. A. Cumulative distribution functions of timing of anterior ipsilateral and within-segment contralateral leg swings, normalized to the phase of the posterior or contralateral lateral leg. Average swing duration of lateral legs is shown by the dashed line, n=5175 strides for ipsilateral phase offsets; n=3809 strides for contralateral offsets. B. Ipsilateral swing timing for each lateral leg in the first and second leg pair, n (strides)=1301 for L2, 1279 for R2, 1317 for L3, 1278 for R3. C. Contralateral swing timing for each left lateral leg, n (strides)=1305 for L1, 1251 for L2, 1253 for L3. D. Cumulative distribution function of timing of contralateral leg swings for rear legs. Average swing duration of rear legs is shown by the dashed line. E. Contralateral swing timing for each rear leg, n (strides)=1530 for L4, 1532 for R4. F. Cumulative distribution functions of timing of anterior ipsilateral and within-segment contralateral leg swings, normalized to the phase of the posterior or contralateral lateral leg. Stance onset of lateral legs is shown by the dashed line, n=4571 strides for ipsilateral stance-swing offsets; n=3548 strides for contralateral stance-swing offsets. G. Ipsilateral swing timing for each lateral leg in the first and second leg pair, compared to stance onset of the reference leg, n (strides)=1145 for L2, 1154 for R2, 1145 for L3, 1127 for R3. H. Contralateral swing timing for after stance initiation of left lateral leg, n (strides)=1203 for L1, 1184 for L2, 1161 for L3.

Supplemental Figure S9

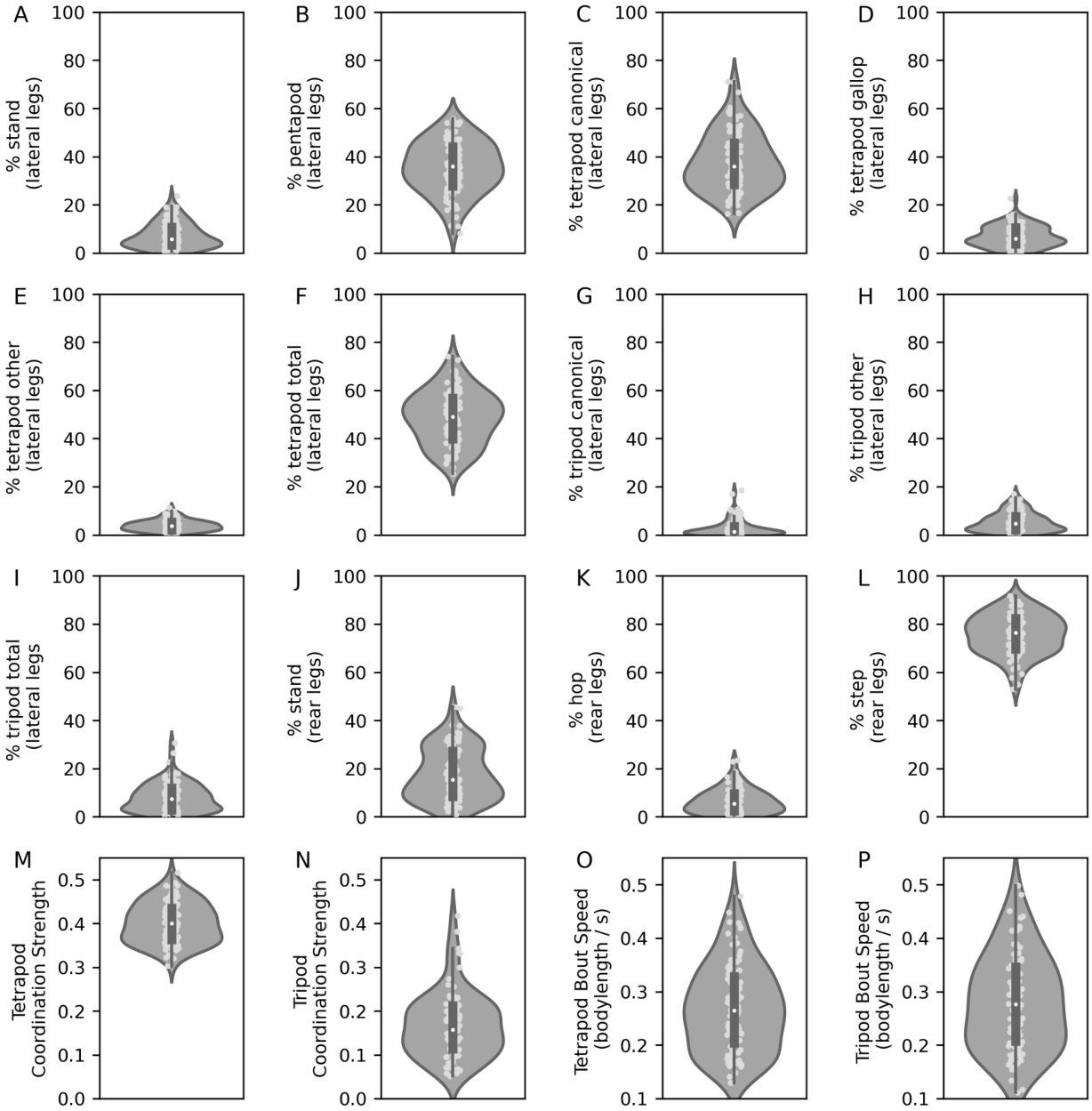

Supplemental Figure S9. Summary of interleg coordination pattern parameters for 103 tardigrades. Each dot represents average data collected from an individual tardigrade.

Supplemental Figure S10

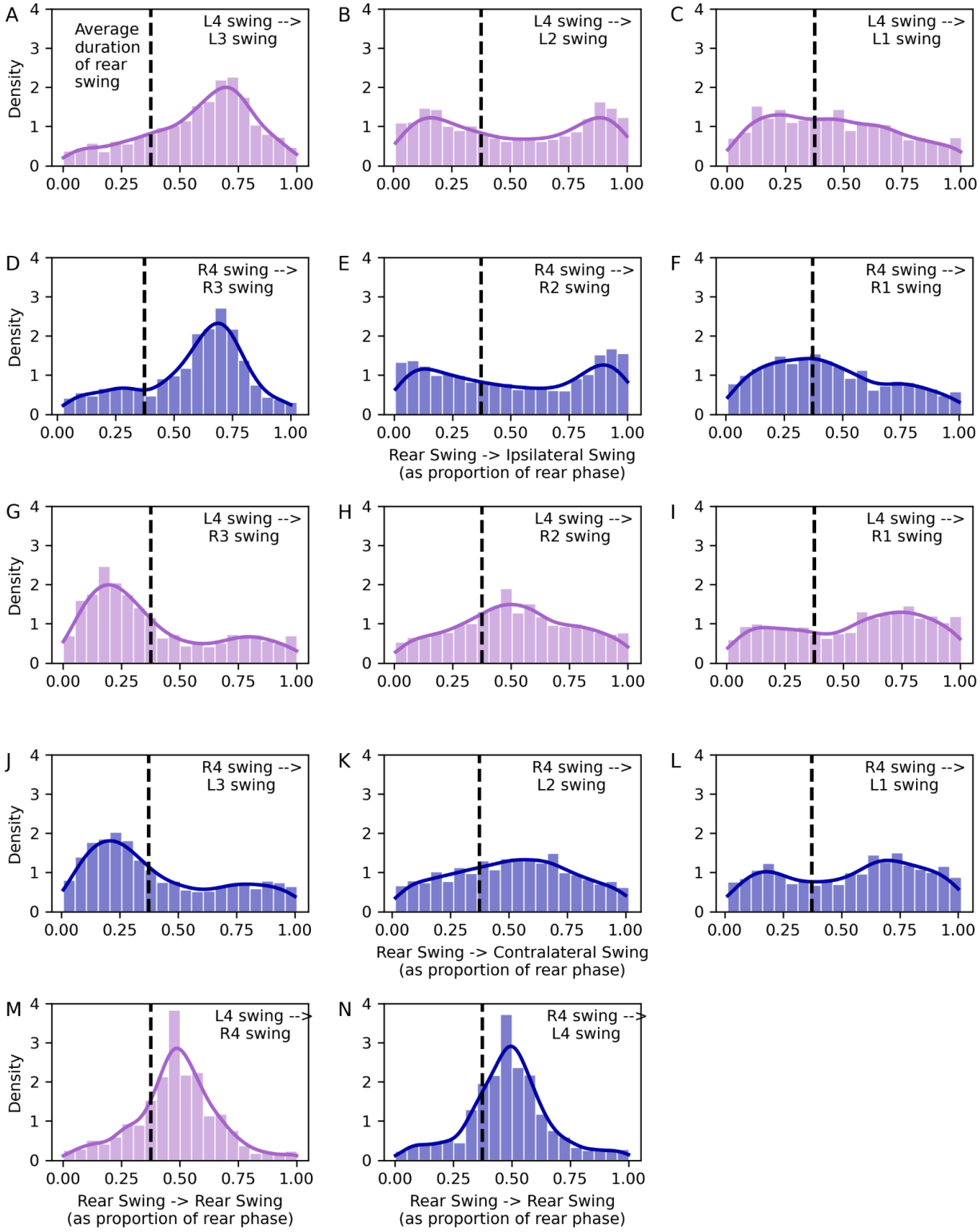

Supplemental Figure S10. Rear leg swings suppress swings of third pair lateral legs. A-L. Probability density distributions of swing initiation phase offsets between the indicated rear leg and the anterior lateral leg, expressed as a fraction of the step period of the rear leg. M-N. Probability density distributions of swing initiation phase offsets between the indicated rear leg and the contralateral rear leg, expressed as a fraction of the step period of the reference rear leg.

Supplemental Movies

Movie S1. Tracking Example

Movie S2. Comparison of locomotion between adult and juvenile *Hypsibius exemplaris*

Movie S3. Comparison of locomotion between adult *Hypsibius exemplaris* and *Ramazzottius*

Movie S4. Comparison of locomotion between control and disulfiram-treated *Hypsibius exemplaris*

Movie S5. Leg tapping and twirling in disulfiram-treated tardigrades